

Running Head: Carbon flow in tropical seascapes

Tracing carbon flow through coral reef food webs using a compound-specific stable isotope approach

Kelton W. McMahon^{1,2,*#}, Simon R. Thorrold², Leah A. Houghton², Michael L. Berumen¹

¹Red Sea Research Center, Division of Biological and Environmental Science and Engineering, King Abdullah University of Science and Technology, Thuwal, 23955, Saudi Arabia

²Biology Department, Woods Hole Oceanographic Institution, Woods Hole, MA 02543, USA

*Author of correspondence: Email: kmcmahon@whoi.edu

#Current address: Ocean Sciences Department, University of California - Santa Cruz, Santa Cruz, CA, 95064, USA

Declaration of Authorship: KWM, SRT, and MLB conceived of and designed the study, KWM and MLB conducted the fieldwork, KWM and LAH conducted the laboratory analyses, KWM and SRT analyzed the data and wrote the manuscript, MLB and LAH revised and edited the manuscript.

Conflict of Interest: The authors declare that they have no conflict of interest.

24 **ABSTRACT**

25 Coral reefs support spectacularly productive and diverse communities in tropical and sub-
26 tropical waters throughout the world's oceans. Debate continues, however, on the degree to
27 which reef biomass is supported by new water column production, benthic primary production,
28 and recycled detrital carbon. We coupled compound-specific $\delta^{13}\text{C}$ analyses with Bayesian
29 mixing models to quantify carbon flow from primary producers to coral reef fishes across
30 multiple feeding guilds and trophic positions in the Red Sea. Analyses of reef fishes with
31 putative diets composed primarily of zooplankton (*Amblyglyphidodon indicus*), benthic
32 macroalgae (*Stegastes nigricans*), reef-associated detritus (*Ctenochaetus striatus*), and coral
33 tissue (*Chaetodon trifascialis*) confirmed that $\delta^{13}\text{C}$ values of essential amino acids from all
34 baseline carbon sources were both isotopically diagnostic and accurately recorded in consumer
35 tissues. While all four source end-members contributed to the production of coral reef fishes in
36 our study, a single source end-member often dominated dietary carbon assimilation of a given
37 species, even for highly mobile, generalist top predators. Microbially-reworked detritus was an
38 important secondary carbon source for most species. Seascape configuration played an important
39 role in structuring resource utilization patterns. For instance, *L. ehrenbergii*, showed a significant
40 shift from a benthic macroalgal food web on shelf reefs ($71 \pm 13\%$ of dietary carbon) to a
41 phytoplankton-based food web ($72 \pm 11\%$) on oceanic reefs. Our work provides insights into the
42 roles that diverse carbon sources play in the structure and function of coral reef ecosystems and
43 illustrates a powerful fingerprinting method to develop and test nutritional frameworks for
44 understanding resource utilization.

45

46 Key words: amino acids; Bayesian mixing model, diet, fish; Red Sea

47

48 **INTRODUCTION**

49 Coral reefs represent some of the most productive and biologically diverse ecosystems on
50 Earth (Odum and Odum 1955; Ryther 1969; Connell 1978; Hughes et al. 2002). Yet this
51 observation remains enigmatic given that many coral reefs occur at latitudes characterized by
52 significant nutrient limitation (Muscatine 1973; Hallock and Schlager 1986). More than a
53 century ago, Darwin (1842) posed the question of how coral reefs were so productive and diverse
54 in oligotrophic ocean waters – a question that we have yet to satisfactorily answer. One
55 hypothesis proposes that reef-associated planktivores act as a “wall of mouths” that captures
56 significant amounts of carbon fixed in the water column by phytoplankton (Emery 1973; Hamner
57 et al. 1988; Genin et al. 2009; Wyatt et al. 2010). Other ideas have linked high productivity on
58 coral reefs to mechanisms that efficiently recycle carbon and nutrients within the system, through
59 symbioses (Muscatine and Porter 1977; Cowen 1988), remineralization pathways (Richter et al.
60 2001; Wild et al. 2004; Wyatt et al. 2012a; de Goeij et al. 2013), and microbially-reworked
61 detrital pathways (Alongi et al. 1988; Gast et al. 1998; Ferrier-Pages and Gattuso 1998).
62 Distinguishing among these competing hypotheses is important to understanding the mechanisms
63 that underlie coral reef function and resilience as well as the species responsible for maintaining
64 these processes in the face of global climate change and anthropogenic disturbance (Pandolfi et
65 al 2003; Cote et al 2005; Hughes et al 2007).

66 The structure and function of coral reefs are intricately tied to the sources and pathways
67 of carbon flow through reef food webs (Lindeman 1942; Moore et al. 2004). However, accurate
68 estimates of carbon flow are challenging to obtain in systems characterized by complex food
69 webs. Stable isotope analysis (SIA) provides a method for tracing carbon flow that avoids many

70 of the challenges associated with constructing food webs from conventional gut content analysis
71 and feeding observations (Deb 1997; Bearhop et al. 2004). However, coral reefs remain
72 challenging systems to examine with SIA due to difficulties characterizing multiple end-
73 members at the base of the food web (hereafter source end-members) and interpreting shifts in
74 diet, trophic position, and baseline isotope values ($\delta^{13}\text{C}_{\text{baseline}}$) in highly dynamic systems (Post
75 2002). Bulk SIA has, therefore, seen limited use in coral reef systems, with most studies either
76 forced to rely on trends of increasing $\delta^{15}\text{N}$ values and decreasing $\delta^{13}\text{C}$ values as indicative of
77 increased reliance on oceanic productivity or suffering from underdetermined mixing models and
78 uncertainty regarding trophic fractionation in complex food webs (Carassou et al. 2008;
79 Greenwood et al. 2010; Wyatt et al. 2012b; Hilting et al. 2013; Letourneur et al. 2013).

80 Recent work has highlighted opportunities to enhance studies of carbon flow in ocean
81 environments by analyzing $\delta^{13}\text{C}$ values of specific biochemical compounds, particularly amino
82 acids (AAs) (reviewed in McMahon et al. 2013). Metabolic diversity in essential AA synthesis
83 pathways and isotope effects generates unique isotopic signatures or “fingerprints” among
84 diverse source end-members (Hayes 2001; Scott et al. 2006; Larsen et al. 2009, 2013) that are
85 robust to many of the factors affecting bulk $\delta^{13}\text{C}$ values (Larsen et al. 2015). While primary
86 producers and bacteria can synthesize essential AAs *de novo*, most animals do not possess the
87 necessary enzymatic pathways to synthesize these AAs at a rate sufficient for normal growth
88 (Borman et al. 1946; Reeds 2000) and therefore must incorporate essential AAs directly from
89 their diet with minimal trophic fractionation (Hare et al. 1991; Howland et al. 2003; Jim et al.
90 2006; McMahon et al 2010). Essential AA $\delta^{13}\text{C}$ signatures propagate through food webs virtually
91 unmodified (Arthur et al. 2014; Schiff et al. 2014; McMahon et al. 2015), which avoids the
92 complications of variable and poorly characterized trophic fractionation factors in mixing models

93 (Bond and Diamond 2011). Furthermore, this compound-specific stable isotope analysis (CSIA)
94 approach typically provides five or more essential AAs with independent synthesis pathways in a
95 single analysis, allowing for better constraint of source end-member signatures while avoiding
96 the biases common to underdetermined mixing models using poorly resolved dual isotope
97 approaches in systems with multiple end-members (Fry 2013; Brett 2014).

98 In this study we coupled CSIA with a Bayesian isotope mixing model approach to
99 determine the sources of carbon assimilated by seven species of coral reef fishes spanning a wide
100 range of feeding guilds and trophic positions on Saudi Arabian reefs in the Red Sea. We initially
101 determined if $\delta^{13}\text{C}$ values in essential AAs differed among four distinct end-members
102 (phytoplankton, benthic macroalgae, corals, and detritus) and between reef locations. We then
103 addressed the following specific questions: 1. Which carbon sources supported our focal reef fish
104 species? 2. Does carbon source use vary spatially between shelf and oceanic reefs? Earlier
105 studies by Emery (1973) and Hamner et al. (1988) hypothesized that water column production
106 contributed significantly to the carbon sequestered in fish biomass on coral reefs, while more
107 recent studies have suggested recycling pathways may play significant roles in reef production
108 (Richter et al. 2001; Wild et al. 2004; de Goeij et al. 2013). As reefs globally face increasing
109 pressures from climate change and anthropogenic disturbances (e.g. Polovina 1984; Arias-
110 Gonzalez et al. 2004; Hilting et al. 2013), understanding carbon flow in reef systems will become
111 even more important to their long term conservation and management.

112

113 **METHODS**

114 *Study site*

115 We sampled four source end-members (96 samples total) and seven coral reef fish
116 species (260 samples total) from isolated coral reefs located on the continental shelf (shelf reefs,
117 $n = 4$) and in oceanic waters beyond the shelf (oceanic reefs, $n = 4$) near Al-Lith on the Saudi
118 Arabian coast of the Red Sea in March 2009 and June 2010 (Fig. 1). The oceanic reefs were
119 steep-walled pinnacles rising rapidly from deep water (>300 m). Shelf reefs were situated on the
120 continental shelf in water not exceeding 60 m depth. Shelf reefs were characterized by water
121 with visibility usually less than 25 m. Conversely, the oceanic reefs were steep-walled pinnacles
122 rising rapidly from deep water (>300 m) with visibility often exceeding 40 m. Saudi reefs in the
123 Red Sea are characterized by relatively little structural complexity at the habitat level (Shepherd
124 and Shepherd 1991), and none of our study reefs had lagoon or back-reef environments.

125 We characterized carbon isotope signatures of four distinct source end-members at the
126 base of the food web on each reef: 1) phytoplankton, 2) macroalgae, 3) coral, and 4) detritus. We
127 collected calanoid copepods that feed on phytoplankton, dinoflagellates, and protists within
128 pelagic food webs (e.g. Kleppel 1993) using a 1 m diameter, 333 μm mesh net towed in the
129 water column around the perimeter of each reef ($n = 3$ tows per reef). Given that essential AAs
130 show virtually no fractionation between diet and consumer (McMahon et al. 2010, 2013), the
131 essential AA $\delta^{13}\text{C}$ values of pelagic copepods provided a faithful proxy for pelagic
132 phytoplankton. We collected a filamentous macroalga (*Womersleyella setacea*) that is farmed by
133 the dusky farmerfish (*Stegastes nigricans*, Lacepede 1802) (Hata and Kato 2002) from each reef
134 ($n = 3$ sites collected throughout each reef). We selected a species of staghorn coral, *Acropora*
135 *pharaonis*, that is targeted by corallivores (e.g., Berumen and Pratchett 2008) to represent carbon
136 fixed by autotrophic zooxanthellae and heterotrophic feeding by corals ($n = 3$ coral tables
137 collected throughout each reef). Given the challenges in isolating the detrital end-member, we

138 selected the detritivorous black sea cucumber, *Holothuria atra*, as a proxy for detritus (Moriarty
139 1982; Uthicke 1999) (n = 3 individuals collected throughout each reef).

140 We collected adult individuals from seven species of reef fishes, representing a suite of
141 feeding guilds from detritivores to top predators. There were no significant differences in total
142 length between individuals collected on shelf and oceanic reefs for any species (Online Resource
143 1). Feeding ecology of each species was classified according to Sommer et al. (1996) and Lieske
144 and Myers (2004). Lined bristletooths, *Ctenochaetus striatus* (Quoy and Gaimard 1825), are
145 common detritivorous surgeonfish that typically ingest sediments to target detritus, blue-green
146 algae, and benthic diatoms. Bullethead parrotfish, *Chlorurus sordidus* (Forsskål 1775), feed on
147 benthic algae and detritus. We sampled two species of damselfish that occupy different feeding
148 guilds. Pale damselfish, *Amblyglyphidodon indicus* (Allen and Randall 2002), feed primarily on
149 zooplankton, while dusky farmerfish, *S. nigricans*, feed almost exclusively on farmed
150 filamentous macroalgae, such as *W. setacea*. Chevron butterflyfish, *Chaetodon trifascialis* (Quoy
151 and Gaimard 1825), are obligate corallivores that feed on the polyps and mucus of corals, most
152 commonly in the genus *Acropora*. Ehrenberg's snapper, *Lutjanus ehrenbergii* (Peters 1869), are
153 mesopredators that feed primarily on benthic invertebrates and small fishes. Giant moray eels,
154 *Gymnothorax javanicus* (Bleeker 1859), were selected as resident top piscivores at each reef.
155 Due to the small size of the reefs, we were able to effectively sample individuals from the entire
156 perimeter of each reef (n = 5 individuals per reef, except *G. javanicus* where two or three
157 individuals were collected per reef).

158 *Sample preparation and analysis*

159 Several calanoid copepods were isolated and then homogenized from each plankton tow.
160 Macroalgae samples were cleaned of epizoic fauna and homogenized. Coral tissue was removed

161 from the skeleton with an air pick and represented a consortium of coral tissue, coral mucus, and
162 the associated microbial community. For the detritus end-member, we used homogenized dermal
163 tissue from *H. atra*. Morays eels were captured in baited fish traps and biopsied with a small
164 hand biopsy tool, while the remaining fish species were collected by spear gun. White muscle
165 samples from all individual fishes were frozen on the boat and transported to an on-shore
166 laboratory for further processing. Samples were frozen at -20°C and then lyophilized (freeze-
167 dried) for 48 hrs prior to homogenization with a mortar and pestle.

168 We acid hydrolyzed and derivatized samples prior to CSIA according to McMahon et al.
169 (2011). Briefly, each sample underwent an acid-catalyzed esterification followed by acylation
170 with trifluoroacetic anhydride (TFAA) and dichloromethane (DCM) under an atmosphere of N₂.
171 Samples were brought up in DCM and injected on column in splitless mode at 260°C and
172 separated on a forte SolGel-1ms column (60 m length, 0.25 mm inner diameter, and 0.25 μm
173 film thickness; SGE Analytical Science, Sydney, Australia) in a Agilent 6890N Gas
174 Chromatograph (GC) at the Woods Hole Oceanographic Institution, Woods Hole, MA, USA.
175 The separated AA peaks were combusted online in a Finnigan gas chromatography-combustion
176 continuous flow interface at 1030°C, then measured as CO₂ on a Thermo Finnigan Mat 253 irm-
177 MS. Standardization of runs was achieved using intermittent pulses of a CO₂ reference gas of
178 known isotopic composition. All CSIA samples were analyzed in duplicate along with AA
179 standards of known isotopic composition from Sigma-Aldrich (mean reproducibility for all
180 individual standard AAs was ± 0.2‰) to correct for the introduction of exogenous carbon and
181 kinetic fractionation associated with derivitization (Silfer et al. 1991). We focused on five
182 essential AAs (threonine, isoleucine, valine, phenylalanine, and leucine) with sufficient peak size

183 and baseline GC separation for accurate CSIA (mean reproducibility for all individuals AAs
184 from a long term lab fish muscle standard was $\pm 0.6\text{‰}$).

185

186 *Data analysis*

187 We characterized unique isotope signatures for the four source end-members on shelf and
188 oceanic reefs based on the $\delta^{13}\text{C}$ values of five essential AAs; threonine, valine, isoleucine,
189 phenylalanine, and leucine. We tested for variations in the $\delta^{13}\text{C}$ values of individual essential
190 AAs using a mixed-model analysis of variance (ANOVA) with end-member ($n = 4$) and location
191 (shelf or oceanic) as fixed factors and reefs nested within location as a random factor. Tukey's
192 honest significant difference (HSD) tests were used for multiple pairwise comparisons of
193 significant effects identified by the ANOVAs. We then visualized the multivariate signatures of
194 essential AA $\delta^{13}\text{C}$ values from source end-members and reef fish species with principal
195 component analysis (PCA) using the covariance matrix.

196 To quantify the relative contributions of the four source end-members to the seven fish
197 species on shelf and oceanic reefs, we used a fully Bayesian stable isotope mixing model
198 approach (sensu Ward et al. 2010) within the Stable Isotope Analysis in R (SIAR) package
199 (Parnell et al. 2010; R development core team 2013, ver. 3.0.2). We used the $\delta^{13}\text{C}$ values of five
200 essential AAs (threonine, isoleucine, valine, phenylalanine, and leucine) to identify unique
201 isotopic signatures for each source end-member on each reef ($n = 3$ samples per end-member per
202 reef). We used a small non-zero trophic discrimination factor in the model ($0.1 \pm 0.1\text{‰}$) that
203 reflected the minimal trophic fractionation of essential AAs between diet and consumer
204 (McMahon et al. 2010). For the consumer data, we used essential AA $\delta^{13}\text{C}$ values from
205 individual samples. We conducted separate models for each species and reef using reef specific

206 end-member essential AA $\delta^{13}\text{C}$ values with the siarsolomcmcv4 function within SIAR (500,000
207 iterations and an initial discard of the first 50,000 iterations as burn-in). We tested for differences
208 in the relative contribution of the dominant source end-member between shelf and oceanic
209 locations for each species with two-sample t-tests ($n = 20$ individuals per location).

210 The resulting data (proportions of each of four end-members) were used to examine
211 variability in carbon source use among focal species and across the seascape. We used a
212 multivariate cluster analysis framework to visualize associations among individual samples and
213 their respective end-member compositions. A k-means strategy identified the most parsimonious
214 number of clusters within the multivariate data set, and then a constellation plot visualized
215 sample associations within these clusters. All univariate, PCA, and cluster analyses were
216 performed in the JMP statistical environment (JMP 2013, ver.11).

217

218 **RESULTS**

219 We quantified $\delta^{13}\text{C}$ values of five essential AAs from a total of 96 end-member samples
220 and 260 fish muscle samples from our eight study reefs (Online Resource 2). Using separate
221 mixed-model univariate ANOVAs of source end-member $\delta^{13}\text{C}$ values for each essential AA, we
222 found a significant location*end-member interaction for Val only (Table 1). Location effects
223 were identified for Thr and Val, while end-members differed significantly for all essential AA
224 values. For Thr and Ile, the coral end-member differed significantly from detritus, which was in
225 turn significantly different from phytoplankton and macroalgae (Tukey's HSD). For Phe, the
226 detritus end-member differed significantly from coral and macroalgae, which were in turn
227 significantly different from phytoplankton. Finally, all four end-members were significantly
228 different for Leu $\delta^{13}\text{C}$ values.

229 We used a PCA of the essential AA $\delta^{13}\text{C}$ values to visualize patterns in the multivariate
230 end-member signatures (Fig. 2). The first two principal components (PCs) of the PCA explained
231 93% of the total variability in the system (PC1 = 70%, PC2 = 23%, Table 2). The loadings for
232 PC1 were all negative and of similar magnitude. Isoleucine was the most important loading for
233 PC2, followed by valine, albeit of opposite sign. The PCA confirmed the relative importance of
234 location and end-members from the univariate ANOVAs above. We found that phytoplankton,
235 macroalgae, coral, and detritus were all clearly separated with non-overlapping 95% density
236 ellipses for almost all end-members from both shelf and oceanic locations in multivariate space
237 (Fig. 2). We detected no obvious effect of location on the multivariate signatures based on the
238 density ellipses for any of the end-members.

239 We then added essential AA $\delta^{13}\text{C}$ data from the seven fish species to the PCA model with
240 the end-member signatures (Table 3) to visualize potential associations between carbon end-
241 members at the base of the reef food webs and upper trophic level consumers (Fig. 3). We found
242 good agreement between end-members and their putative consumers. The herbivorous
243 damselfish, *S. nigricans*, always grouped near the macroalgal end-member, *C. striatus* were
244 grouped with the detritus end-member, and *C. trifascialis* were grouped with the coral end-
245 member. The putative planktivore, *A. indicus*, grouped with the phytoplankton end-member on
246 oceanic reefs, however, individuals on shelf reefs fell between phytoplankton and macroalgae.
247 Individuals from the remaining fish species generally fell in the multivariate space between the
248 end-members, indicating that we had adequately constrained the carbon sources at the base of the
249 food web for all of the focal species.

250 The excellent separation of source end-members in multivariate space, good agreement
251 between essential AA $\delta^{13}\text{C}$ values of end-members and their primary consumers, and the lack of

252 trophic fractionation of essential AAs provided strong justification for the use of an isotope
253 mixing model to quantify the relative contributions of source end-members to reef fish
254 consumers. The Bayesian isotope mixing model revealed significant variability in the relative
255 contributions of source end-members to upper trophic level consumers (Fig. 4). Variance in
256 model output after 500,000 iterations of the SIAR mixing model was small ($5 \pm 3\%$; Online
257 Resource 3).

258 Each of the four source end-members contributed the majority of the carbon assimilated
259 by at least one of the seven fish species across the seascape (Fig. 4). Carbon sources for our
260 primary end-member consumers were generally dominated by their putative diet. Detritus,
261 macroalgae, and coral were the dominant source end-members for *C. striatus* (shelf = $76 \pm 8\%$,
262 oceanic = $70 \pm 10\%$), *S. nigrigans* (shelf = $78 \pm 10\%$, oceanic = $72 \pm 11\%$), and *C. trifascialis*
263 (shelf = $83 \pm 4\%$, oceanic = $79 \pm 5\%$), respectively. There was no effect of location on primary
264 carbon source contribution for any of the three species (samples pooled across reefs within
265 location, two sample t-test, $p > 0.05$). Phytoplankton production contributed $57 \pm 7\%$ to our
266 putative planktivore, *A. indicus*, on shelf reefs but that proportion increased significantly to $87 \pm$
267 5% on oceanic reefs (two sample t-test, $t_{38} = -15.49$, $p < 0.0001$). Detritus (shelf = $49 \pm 14\%$,
268 oceanic = $44 \pm 10\%$) and macroalgae (shelf $36 \pm 16\%$, oceanic = $34 \pm 12\%$) were both major
269 contributors to the diet of *C. sordidus*, with no significant differences between locations for
270 either carbon source. However, carbon source contributions for both *L. ehrenbergii* and *G.*
271 *javanicus* showed significant differences between shelf and oceanic reefs. Macroalgal carbon
272 contributed the majority ($71 \pm 13\%$) of the carbon to *L. ehrenbergii* on shelf reefs, but only $17 \pm$
273 10% on oceanic reefs (two sample t-test, $t_{38} = 14.4$, $p < 0.0001$). Phytoplankton was the
274 dominant end-member ($72 \pm 11\%$) for *L. ehrenbergii* on the oceanic reefs. While phytoplankton

275 was the dominant end-member for *G. javanicus* across locations, contributions were significantly
276 higher on oceanic reefs ($79 \pm 9\%$) than on shelf reefs ($64 \pm 10\%$) (two sample t-test, $t_{38} = -3.66$,
277 $p = 0.002$).

278 We used cluster analysis of end-member utilization followed by a constellation plot to
279 help visualize patterns of carbon flow from source end-members to focal consumers. A k-means
280 cluster analyses identified six clusters as the most parsimonious grouping of multivariate end-
281 member proportions. The resulting constellation plot revealed that each of the individual carbon
282 source end-members dominated one of the six clusters (Fig. 5). Cluster A consisted of
283 individuals with high proportions (mean \pm SD) of the macroalgal end-member ($75 \pm 9\%$), and
284 included *S. nigricans* (Sni) from both shelf and oceanic reefs as well as *L. ehrenbergii* (Leh)
285 from shelf reefs. Samples in Cluster B contained relatively high proportions of both detritus (45
286 $\pm 10\%$) and macroalgae ($36 \pm 10\%$) and were dominated taxonomically by *C. sordidus* (Sor), but
287 also contained several individuals of *C. striatus* (Cst), *L. ehrenbergii*, and *S. nigricans*. Cluster C
288 was composed predominantly of *C. striatus* samples with high proportions of detritus ($74 \pm 8\%$),
289 while Cluster D consisted exclusively of *C. trifascialis* (Ctr) individuals and the coral end-
290 member ($75 \pm 9\%$). Cluster E contained the phytoplankton end-member ($79 \pm 9\%$) and contained
291 a taxonomically diverse representation of *A. indicus* (Ain) and *L. ehrenbergii* samples from
292 oceanic reefs, and *G. javanicus* (Gja) samples from both oceanic and shelf locations. Finally,
293 Cluster F consisted almost entirely of *A. indicus* and *L. ehrenbergii* individuals from shelf reefs
294 that were characterized by approximately equal proportions of phytoplankton ($55 \pm 7\%$) and
295 macroalgal ($38 \pm 7\%$) end-members.

296

297 **DISCUSSION**

298 Identifying important carbon sources supporting coral reef food webs remains a
299 significant and ongoing challenge to ocean ecologists (Wyatt et al. 2012b; Hilting et al. 2013;
300 Letourneur et al. 2013). However, the CSIA fingerprinting approach that we outline here has
301 considerable potential to provide a more comprehensive assessment of carbon flow through reef
302 food webs than was previously possible. We found excellent separation in the $\delta^{13}\text{C}$ values of
303 essential AAs among four important source end-members (phytoplankton, macroalgae, coral,
304 and detritus) on the study reefs. We were then able to use Bayesian isotope mixing models to
305 determine relative contributions of each of the end-members to a group of reef fishes spanning
306 multiple feeding guilds and trophic positions. The method provided an alternative to
307 conventional dual-isotope (carbon and nitrogen) approaches that are often under-determined in
308 complex food webs with multiple end-members (Fry 2013; Brett 2014). Moreover, by using
309 essential AAs that exhibit minimal fractionation across trophic levels this method avoids
310 complications of variable and poorly characterized trophic fractionation factors in mixing models
311 (Bond and Diamond 2011). The CSIA fingerprinting approach therefore affords the ability to test
312 hypotheses concerning the response of carbon flow through reef food webs to processes
313 including both natural and anthropogenic disturbances and climate change.

314 We tested the CSIA fingerprinting approach used here by estimating carbon source
315 contributions for several species of coral reef fishes with well-constrained diets. For instance, we
316 estimated that the obligate corralivorous butterflyfish, *C. trifascialis*, received $81 \pm 5\%$ of its
317 carbon from coral-fixed carbon. Similarly, the farming damselfish, *S. nigricans*, received $75 \pm$
318 11% of its dietary carbon from macroalgae. Macroalgae were also important carbon sources for a
319 number of other species in our study, including the roaming herbivore (*C. sordidus*) on oceanic
320 and shelf reefs, and the mesopredator (*L. ehrenbergii*) and the planktivorous damselfish (*A.*

321 *indicus*) on shelf reefs only. Microbially-reworked detritus dominated the sources of essential
322 AAs to *C. striatus*, as we predicted. Interestingly, a recent study has suggested that despite its
323 dental morphology, *C. striatus* can remove more algal turf per hour than the common
324 herbivorous grazer *Acanthurus nigrofuscus* (Marshall and Mumby 2012). We found some
325 support for the functional role of *C. striatus* as an algal grazer, with macroalgae providing an
326 average of $14 \pm 7\%$ (upwards of 30% for some individuals) of the carbon consumed and
327 assimilated by individuals across the seascape.

328 Water column primary production represents a significant source of energy and nutrients
329 for coral reefs, as well as an important link between oceanic and reef ecosystems (Emery 1973;
330 Hamner et al. 1988; Richter et al. 2001; Genin et al 2002). Three of the seven species in our
331 study, the planktivorous damselfish *A. indicus*, the mesopredator *L. ehrenbergii*, and the top
332 predator *G. javanicus*, received significant amounts of carbon fixed by phytoplankton ($60 \pm$
333 28%). Interestingly, two dominantly herbivorous fishes, *C. sordidus* and *S. nigricans*, showed
334 moderate reliance on phytoplankton-based carbon ($13 \pm 6\%$, reaching 30% for some individuals)
335 on oceanic reefs. Previous studies have found that nominal herbivores such as *Stegastes spp.*
336 assimilated at least some carbon from oceanic sources based on bulk SIA (Wyatt et al. 2012b;
337 Letourneur et al. 2013). Both Wyatt et al. (2012b) and Letourneur et al. (2013) hypothesized that
338 the link between the oceanic production signal and herbivores was through changes in nutrient
339 sources supporting macroalgal production associated with oceanographic forcing, such as
340 upwelling of nutrients (Wyatt et al. 2012a). We were able to directly attribute the oceanic
341 production signal in the herbivorous *S. nigricans* and *C. sordidus* in our study to assimilation of
342 phytoplankton production. Herbivores often consume significant numbers of demersal
343 crustaceans that live in benthic reef habitats (Kramer et al. 2013), either incidentally or as a

344 complimentary feeding strategy to cope with low protein, plant-based diets (Cruz-Rivera and
345 Hay 2000; Raubenheimer et al. 2009). Many of these crustaceans move up into the water column
346 at night to feed on phytoplankton and particulate organic matter, thereby providing another
347 mechanism for transferring carbon fixed in the water column to herbivorous reef fishes.
348 Alternatively, we cannot rule out the possibility that these consumers were feeding on benthic
349 diatoms, as the amino acid fingerprints of benthic diatoms have not been explicitly tested.
350 Certainly, more detailed studies will be needed to fully resolve the processes that link
351 phytoplankton production with reef food webs.

352 Detritus represents a major carbon pool in coral reef systems (Crossman et al. 2001), yet
353 decomposition processes are not well understood as they are generally more diverse and difficult
354 to measure than production processes (Alongi 1988; Moore et al. 2004). The CSIA fingerprinting
355 approach outlined here provides a method for identifying microbial processing of organic
356 material (McCarthy et al. 2004; Larsen et al. 2013), and therefore has the potential to improve
357 our understanding of the role that detrital organic material plays in coral reef trophic dynamics
358 and productivity. Sampling the detrital end-member, however, is often difficult in reef
359 environments (e.g. Hilting et al. 2013). We used a detritivorous sea cucumber (Moriarty 1982;
360 Uthicke 1999), *H. atra*, to constrain the isotopic end-member for carbon that had been
361 reprocessed by microbial activity through detrital pathways. The essential AA $\delta^{13}\text{C}$ signatures of
362 *H. atra* matched closely to the heterotrophic bacteria end-member of Larsen et al. (2013),
363 suggesting that the sea cucumbers were feeding on a food source that had undergone substantial
364 microbial reworking (Online Resource 4). In addition, our analyses found that detritus was the
365 primary source end-member ($73 \pm 9\%$) for the surgeonfish *C. striatus* across the entire system.
366 Previous work indicates that *C. striatus* feeds extensively on detritus based on dental

367 morphology and feeding observations (Choat et al. 2002, 2004). Taken together, these results
368 suggest that while a combination of new reef and water column production may have been the
369 original source of organic matter to reef detritus, the essential AA $\delta^{13}\text{C}$ signature of *H. atra*
370 adequately constrained the isotopic signature of the detrital end-member that is distinct from
371 newly-fixed phytoplankton, macroalgae, and coral carbon.

372 Detritus was an important source of essential AAs for several focal species, particularly
373 on shelf reefs. For instance, we found that *C. sordidus* received nearly half of its dietary carbon
374 from a detrital end-member with the remaining carbon coming largely from macroalgae. Despite
375 being one of the most abundant coral reef fishes in the Red Sea, the feeding ecology of *C.*
376 *sordidus* has been challenging to define. Some studies have described *C. sordidus* as a roaming
377 herbivore (Chen 2002; Ledlie et al. 2007; Lecchini and Poignonec 2009), while others have
378 suggested that *C. sordidus* is better described as a detritivore (Choat et al. 2002, 2004). Our
379 results indicated that *C. sordidus* relied on both new reef-derived macroalgal production and
380 microbially-reworked detritus, exhibiting significant dietary plasticity at the individual level.
381 Several upper trophic level consumers, including the mesopredator *L. ehrenbergii* and the top
382 predator *G. javanicus*, received an average of $14 \pm 10\%$ (reaching 45% for some individuals) of
383 their dietary carbon from detritus on shelf reefs. These results support the findings of a previous
384 study using bacteria-specific fatty acid profiles and bulk SIA that highlighted the importance of
385 detrital organic matter to the production of the mesopredator *Lethrinus nebulosus* in Australia
386 (Wyatt et al. 2012b). Overall, these results suggest conventional methods of assessing resource
387 utilization of coral reef fishes likely underestimate the importance of microbially-recycled
388 carbon fueling coral reef food webs.

389 While all four source end-members contributed to the production of upper trophic level
390 coral reef fishes in our study, we found that a single source end-member often dominated dietary
391 carbon assimilation in several focal species. This is perhaps not surprising for primary or even
392 secondary consumers, such as the obligate coralivore *C. trifascialis*, the farming herbivore *S.*
393 *nigricans*, and the detritivore *C. striatus*, that are closely linked to their respective end-members
394 at the base of the food web. It has been far more challenging to determine if upper trophic level
395 consumers are similarly linked to a single source end-member at the base of the food web.
396 Conventional diet and bulk isotope approaches typically require extensive characterization of all
397 dietary linkages within a food web to accurately determine the relative contribution of source
398 end-members to top predators. The amino acid isotope fingerprinting approach that we used to
399 track carbon assimilation patterns, on the other hand, does not require reconstruction of entire
400 food web to accurately identify baseline carbon sources for top predators. We found that high
401 trophic level predators in our study system, *L. ehrenbergii* and *G. javanicus*, received the vast
402 majority (>70%) of their carbon from a single end-member, indicating the presence of tightly
403 linked food chains on coral reefs. This result was surprising given that these predators and their
404 typical prey are all highly mobile generalists with the ability to mix diets across multiple food
405 webs (Sommer et al. 1996; Lieske and Myers (2004). These newly discovered tightly-link food
406 webs open new questions about the resilience of top predators to disturbances at the base of the
407 food web.

408 We found significant plasticity in carbon flow patterns of food webs supporting several
409 species in our system as a function of foraging location within the seascape. For instance, when
410 foraging on shallow reefs on the continental shelf, *L. ehrenbergii* relied heavily on reef-derived
411 production from macroalgae and detritus (>85%). Yet when foraging on oceanic reefs

412 surrounded by deep open water, *L. ehrenbergii* received the majority of their dietary carbon from
413 new water column-based production (>70%), with less than 20% coming from macroalgae and
414 detritus. This pattern of increased reliance on phytoplankton production in oceanic food webs
415 was apparent in several other species as well. The putative planktivore *A. indicus* always relied
416 on water column-based phytoplankton production for the majority of its dietary carbon; however,
417 individuals residing on shelf reefs also received significant contributions ($37 \pm 10\%$) of dietary
418 carbon from macroalgal sources. The mix of phytoplankton and algae in the diet of *A. indicus* on
419 shelf reefs likely reflected higher particulate organic matter loads in the water column of these
420 shallow water shelf reefs, though it is possible that *A. indicus* was directly ingesting macroalgae
421 or macroalgae-consuming invertebrates from the reef surface on the shelf reefs (e.g. Lammens et
422 al. 1985). Yet, as was the case with *L. ehrenbergii*, *A. indicus* residing on oceanic reefs were
423 dominated by carbon from phytoplankton production ($87 \pm 5\%$). A similar case was seen in the
424 top predator *G. javanicus*, where the importance of water column-based phytoplankton
425 production was significantly higher on oceanic reefs ($79 \pm 9\%$) than it was for individuals on
426 shelf reefs ($64 \pm 10\%$). These patterns could not be explained by consumer size, as there were no
427 significant differences in total fish length between individuals collected on shelf and oceanic
428 reefs for any species.

429 Previous research based on patterns of increasing bulk $\delta^{15}\text{N}$ values and decreasing $\delta^{13}\text{C}$
430 values in many coral reef fishes has suggested that the importance of oceanic derived production
431 to coral reef food webs often increases with proximity to the open ocean, perhaps related to the
432 increased access to oceanic nutrients (Wyatt et al. 2012b; Hilting et al. 2013; Letourneur et al.
433 2013). We directly quantified the increase in relative contribution of water column-based
434 phytoplankton production to a diverse set of upper trophic level coral reef fishes as a function of

435 reef location within the seascape. However, further research is needed to determine whether the
436 observed increase in reliance on water-column production for fishes on oceanic reefs reflected a
437 dietary switch to a more phytoplankton-based food web or an increase in the flow of
438 phytoplankton carbon through the same food webs as on shelf reefs. While our study targeted
439 adult individuals across the entire seascape, previous work has shown that ontogenetic shifts in
440 habitat usage of coral reef fishes can also result in dramatic changes in resource utilization
441 through time and space (McMahon et al. 2012; Cocheret de la Moriniere et al 2013).

442 In conclusion, we found that phytoplankton, macroalgae, coral, and detritus-based carbon
443 sources were all important in supporting the production of a diverse suite of fishes on coral reefs
444 of the Red Sea. However, seascape configuration played an important role in structuring the
445 resource utilization patterns of several species in our study, including a numerically dominant
446 planktivore, a commercially important mesopredator, and a piscivorous top predator. Moreover,
447 carbon utilization in several upper trophic level consumers was dominated by a single end-
448 member, indicating tight links from a single group of primary producers at the base of a food
449 web to top predators. Further work addressing a larger number of species is needed to more
450 comprehensively understand the flow of carbon through entire coral reef food webs. Nonetheless
451 the ability to determine end-member contributions to carbon assimilation in reef fishes using
452 CSIA fingerprinting provides a powerful method to develop and test nutritional frameworks for
453 analyzing resource acquisition and allocation. Understanding these trophodynamic interactions is
454 a key to understanding the spatial resilience of complex ecosystems, such as coral reefs.

455

456 **ACKNOWLEDGEMENTS**

457 This research was based on work supported by Awards USA 00002 and KSA 00011 from King

458 Abdullah University of Science and Technology (KAUST); additional funding was provided by
459 the Woods Hole Oceanographic Institution (WHOI), a KAUST-WHOI award (SPCF-
460 7000000104), and KAUST baseline research funds. We thank E. Mason and the Dream Divers
461 crew for boat and dive operation support, C. Braun for creating the site map, and the following
462 people for field assistance: C. Braun, T. Sinclair-Taylor, M. Priest, G. Nanninga, N. desRosiers,
463 P. de la Torre, J. Bouwmeester, L.-L. Hamady. We also thank two anonymous reviewers and the
464 handling editor for valuable comments on this paper.

465

466 **LITERATURE CITED**

467 Alongi DM (1988) Detritus in coral reef ecosystems: fluxes and fates. Proc 6th Int Coral Reef
468 Symp 1:29-36.

469 Arias-Gonzalez JE, Nunez-Lara E, Gonzalez-Salas C, Galzin R (2004) Trophic models for
470 investigation of fishing effect on coral reef. Ecol Model 172:197-212

471 doi:10.1016/j.ecolmodel.2003.09.007

472 Arthur KW, Kelez S, Larsen T, Choy CA, Popp BN (2014) Tracing the biosynthetic source of
473 essential amino acids in marine turtles using $\delta^{13}\text{C}$ fingerprints. Ecology 95:1285-1293

474 doi:10.1890/13-0263.1

475 Bearhop S, Adams CE, Waldron S, Fuller RA, Macleod H (2004) Determining trophic niche
476 width: a novel approach using stable isotope analysis. J Anim Ecol 73:1007-1012

477 doi:10.1111/j.0021-8790.2004.00861.x

478 Berumen ML, Pratchett MS (2008) Trade-offs associated with dietary specialisation for

479 corallivorous butterflyfishes. Behav Ecol Sociobiol 62:989-994 doi: 10.1007/s00265-

480 007-0526-8

- 481 Bond AL, Diamond AW (2011) Recent Bayesian stable-isotope mixing models are highly
482 sensitive to variation in discrimination factors. *Ecol App* 21:1017-1023 doi:10.1890/09-
483 2409.
- 484 Borman A, Wood TR, Black HC, Anderson EG, Oesterling MJ, Womack M, Rose WC (1946)
485 The role of arginine in growth with some observations on the effects of argininic acid. *J*
486 *Biol Chem* 166:585-594
- 487 Brett MT (2014) Resource polygon geometry predicts bayesian stable isotope mixing model
488 bias. *Mar Ecol Prog Ser* 514:1-12 doi:10.3354/meps11017
- 489 Carassou L, Kulbicki M, Nicola TJR, Polunin NVC (2008) Assessment of fish trophic status and
490 relationships by stable isotope data in the coral reef lagoon of New Caledonia, southwest
491 Pacific. *Aquat Living Resour* 21:1-12 doi:10.1051/alr:2008017
- 492 Chen L-S (2002) Post-settlement diet shift of *Chlorurus sordidus* and *Scarus schlegeli* (Pisces:
493 Scaridae). *Zool Stud* 41:47-58
- 494 Choat JH, Clements KD, Robbins WD (2002) The trophic status of herbivorous fishes on coral
495 reefs. I. Dietary analyses. *Mar Biol* 140:613-623 doi:10.1007/s00227-001-0715-3
- 496 Choat JH, Robbins WD, Clements KD (2004) The trophic status of herbivorous fishes on coral
497 reefs. II. Food processing modes and trophodynamics *Mar Biol* 145:445-454
498 doi:10.1007/s00227-004-1341-7
- 499 Cocheret de la Moriniere E, Pollux BJA, Nagelkerken I, Hemminga MA, Huiskes AHL, van der
500 Velde G (2003) Ontogenetic dietary changes of coral reef fishes in the mangrove-
501 seagrass-reef continuum: stable isotopes and gut-content analysis. *Mar Ecol Prog Ser*
502 246:279–289 doi:10.3354/meps246279
- 503 Connell JH (1978) Diversity in tropical rain forests and coral reefs. *Science* 199:1302–1310

- 504 Cote IM, Gill JA, Gardner GA, Watkinson AR (2005) Measuring coral reef decline through
505 meta-analysis. *Philos Trans Roy Soc Lond B Biol Sci* 360:385-395 DOI: 10.1098/rstb.2004.1591
- 506 Cowen R (1988) The role of algal symbiosis in reefs through time. *Palaios* 3:221-227
507 doi:10.2307/3514532
- 508 Crossman DJ, Choat JH, Clements KD, Hardy T, McConochie J (2001) Detritus as food for
509 grazing fishes on coral reefs. *Limnol Oceanogr* 46:1596-1605
- 510 Cruz-Rivera E, Hay ME (2000) The effects of diet mixing on consumer fitness: macroalgae,
511 epiphytes, and animal matter as food for marine amphipods. *Oecologia* 123:252-264
512 doi:10.1007/s004420051012
- 513 Darwin C (1842) *The Structure and Distribution of Coral Reefs*. Appleton and Co., New York.
- 514 de Goeij JM, van Oevelen D, Vermeij MJ, Osinga R, Middelburg JJ, de Goeij AF, Admiraal W
515 (2013) Surviving in a marine desert: the sponge loop retains resources within coral reefs.
516 *Science* 342:108-110 doi:10.1126/science.1241981
- 517 Deb D (1997) Trophic uncertainty vs parsimony in food web research. *Oikos* 78:191-194
- 518 Emery A (1973) Comparative ecology and functional osteology of fourteen species of damselfish
519 (*Pices*: Pomacentridae) at Alligator Reef, Florida Keys. *Bull Mar Sci* 23:649-770
- 520 Ferrier-Pages C, Gattuso JP (1998) Biomass, production and grazing rates of pico- and
521 nanoplankton in coral reef waters (Miyako Island, Japan). *Microb Ecol* 35:46-57
- 522 Fry B (2013) Alternative approaches for solving underdetermined isotope mixing problems. *Mar*
523 *Ecol Prog Ser* 472:1–13 doi:10.3354/meps10168
- 524 Gast GJ, Wiegman S, Wieringa E, Van Duyl FC, Bak RPM (1998) Bacteria in coral reef water
525 types: Removal of cells, stimulation of growth and mineralization. *Mar Ecol Prog Ser*
526 167:37-45

- 527 Genin A, Monismith SG, Reidenbach MA, Yahel G, Koseff JR (2009) Intense benthic grazing of
528 phytoplankton in a coral reef. *Limnol Oceanogr* 54:938-951
529 doi:10.4319/lo.2009.54.3.0938
- 530 Greenwood NDW, Sweeting CJ, Polunin NVC (2010) Elucidating the trophodynamics of four
531 coral reef fishes of the Solomon Islands using $\delta^{15}\text{N}$ and $\delta^{13}\text{C}$. *Coral Reefs* 29:785-792
532 doi:10.1007/s00338-010-0626-1
- 533 Hallock P, Schlager W (1986) Nutrient excess and demise of coral reefs and carbonate platforms.
534 *Palaios* 1:389-398
- 535 Hamner WM, Jones MS, Carleton JH, Hauri IR, Williams DM (1988) Zooplankton,
536 planktivorous fishes, and water currents on a windward reef face: Great Barrier Reef,
537 Australia. *Bull Mar Sci* 42:459-479
- 538 Hare PE, Fogel ML, Stafford TW, Mitchell AD, Hoering TC (1991) The isotopic composition of
539 carbon and nitrogen in individual amino acids isolated from modern and fossil proteins. *J*
540 *Archaeol Sci* 18:277-292 doi:10.1016/0305-4403(91)90066-X
- 541 Hata H, Kato M (2002) Weeding by the herbivorous damselfish *Stegastes nigricans* in nearly
542 monocultural algae farms. *Mar Ecol Prog Ser* 237:227–231 doi:10.3354/meps237227
- 543 Hayes JM (2001) Fractionation of the Isotopes of Carbon and Hydrogen in Biosynthetic
544 Processes. In: Cole DR, Valley JW (eds) *Reviews in Mineralogy and Geochemistry* 43,
545 *Stable Isotope Geochemistry*. The Mineralogical Society of America, Washington, pp
546 225–277
- 547 Hedges JJ, Baldock JA, Gelinas Y, Lee C, Peterson ML, Wakeham SG (2001) Evidence for non-
548 selective preservation of organic matter in sinking marine particles. *Nature* 409:801-804
549 doi:10.1038/35057247

- 550 Hilting AK, Currin CA, Kosaki RK (2013) Evidence for benthic primary production support of
551 an top predator-dominated coral reef food web. *Mar Biol* 160:1681-1695
552 doi:10.1007/s00227-013-2220-x
- 553 Howland MR, Corr LT, Young SMM, Jones V, Jim S, van der Merwe NJ, Mitchell AD,
554 Evershed RP (2003) Expression of the dietary isotope signal in the compound-specific
555 $\delta^{13}\text{C}$ values of pig bone lipids and amino acids. *Int J Osteoarchaeol* 13:54-65
556 doi:10.1002/oa.658
- 557 Hughes TP, Bellwood DR, Connolly SR (2002) Biodiversity hotspots, centres of endemism, and
558 the conservation of coral reefs. *Ecol Lett* 5:775-784 doi:10.1046/j.1461-
559 0248.2002.00383.x
- 560 Hughes TP, Rodrigues MJ, Bellwood DR, Ceccarelli D, Hoegh-Guldberg O, McCook L,
561 Moltchanivskyj N, Pratchett MS, Steneck RS, Willis B (2007) Phase shifts, herbivory,
562 and the resilience of coral reefs to climate change. *Curr Biol* 17:360-365
563 doi:10.1016/j.cub.2006.12.049
- 564 Jim S, Jones V, Ambrose SH, Evershed RP (2006) Quantifying dietary macronutrient sources of
565 carbon for bone collagen biosynthesis using natural abundance stable carbon isotope
566 analysis. *Br J Nutr* 95:1055-1062 doi: DOI:10.1079/BJN20051685
- 567 JMP 2013. Graphic builder, version 11. SAS Institute Inc., Cary, NC, URL
568 <http://www.jmp.com/software/jmp>.
- 569 Kleppel, GS (1993) On the diets of calanoid copepods. *Mar Ecol Prog Ser* 99:183-195
- 570 Kramer MJ, Bellwood O, Bellwood DR (2013) The trophic importance of algal turfs: the
571 crustacean link. *Coral Reefs* 32:575-583 doi:10.1007/s00338-013-1009-1
- 572 Lammens EHRR, de Nie HW, Vijverberg J, van Densen WLT (1985) Resource partitioning and

- 573 niche shifts of bream (*Abramis brama*) and eel (*Anguilla Anguilla*) mediated by predation
574 of smelt (*Osmerus eperlanus*) on *Daphnia hyaline*. Can J Fish Aquat Sci 42:1342-1351
575 doi:10.1139/f85-169
- 576 Letourneur Y, Lison De Loma T, Richard P, Harmelin-Vivien ML, Cresson P, Banaru D,
577 Fontaine MF, Gref T, Planes S (2013). Identifying carbon sources and trophic position of
578 coral reef fishes using diet and stable isotope ($\delta^{15}\text{N}$ and $\delta^{13}\text{C}$) analyses in two contrasted
579 bays in Moorea, French Polynesia. Coral Reefs 32:1091-1102 doi:10.1007/s00338-013-
580 1073-6
- 581 Larsen T, Bach LT, Salvattecchi R, Wang YV, Andersen N, Ventura M, McCarthy MD (2015)
582 Assessing the potential of amino acid $\delta^{13}\text{C}$ patterns as a carbon source tracer in marine
583 sediments: effects of algal growth conditions and sedimentary diagenesis. Biogeosci
584 Discuss 12:1613-1351 doi:10.5194/bgd-12-1613-2015
- 585 Larsen T, Taylor DL, Leigh MB, O'Brien DM (2009) Stable isotope fingerprinting: a novel
586 method for identifying plant, fungal, or bacterial origins of amino acids. Ecology
587 90:3526-3535 doi:10.1890/08-1695.1
- 588 Larsen T, Ventura M, Andersen N, O'Brien DM, Piatowski U, McCarthy MD (2013) Tracing
589 carbon sources through aquatic and terrestrial food webs using amino acid stable isotope
590 fingerprinting. PLoS ONE e73441 doi:10.1371/journal.pone.0073441
- 591 Lecchini D, Poignonec D (2009) Spatial variability of ontogenetic patterns in habitat associations
592 by coral reef fishes (Moorea lagoon–French Polynesia). Est Coast Shelf Sci 82:553-556
593 doi:10.1016/j.ecss.2009.01.023
- 594 Ledlie MH, Graham NAJ, Bythell JC, Wilson SK, Jennings S, Polunin NVC, Hardcastle J (2007)
595 Phase shifts and the role of herbivory in the resilience of coral reefs. Coral Reefs

- 596 26:6411-653 doi:10.1007/s00338-007-0230-1
- 597 Lieske E, Myers RF (2004) Coral Reef Guide: Red Sea. Harper Collins, Oxford, UK.
- 598 Lindeman RL (1942) The trophic-dynamic aspect of ecology. Ecology 23:399-417
- 599 doi:10.2307/1930126
- 600 Marshall A, Mumby PJ (2012) Revisiting the functional roles of the surgeonfish *Acanthurus*
- 601 *nigrofuscus* and *Ctenochaetus striatus*. Coral Reefs 31:1093-1101 doi:10.1007/s00338-
- 602 012-0931-y
- 603 McCarthy DM, Benner R, Lee C, Hedges JL, Fogel ML (2004) Amino acid carbon isotopic
- 604 fractionation patterns in oceanic dissolved organic matter: an unaltered photoautotrophic
- 605 source for dissolved organic nitrogen in the ocean? Mar Chem 92:123-134
- 606 doi:10.1016/j.marchem.2004.06.021
- 607 McMahon KW, Fogel ML, Elsdon T, Thorrold SR (2010) Carbon isotope fractionation of amino
- 608 acids in fish muscle reflects biosynthesis and isotopic routing from dietary protein. J
- 609 Anim Ecol 79:1132-1141 doi:10.1111/j.1365-2656.2010.01722.x
- 610 McMahon KW, Fogel ML, Johnson BJ, Houghton LA, Thorrold SR (2011) A new method to
- 611 reconstruct fish diet and movement patterns from $\delta^{13}\text{C}$ values in otolith amino acids. Can
- 612 J Fish Aquat Sci 68:1330-1340 doi:10.1139/f2011-070
- 613 McMahon KW, Berumen ML, Thorrold SR (2012) Linking habitat mosaics and connectivity in a
- 614 coral reef seascape. Proc Natl Acad Sci (USA) 109:15372-15376
- 615 doi:10.1073/pnas.1206378109
- 616 McMahon KW, Hamady L-L, Thorrold SR (2013) Ocean ecogeochemistry – A review.
- 617 Oceanogr Mar Biol: Ann Rev 51:327-374
- 618 McMahon KW, Polito M, Abel S, McCarthy MD, Thorrold SR (2015) Carbon and nitrogen

- 619 isotope fractionation of amino acids in an avian marine predator, the gentoo penguin
620 (*Pygoscelis papua*). *Ecol Evol* 5:1278-1290 doi:10.1002/ece3.1437.
- 621 Moore JC, Berlow EL, Coleman DC, de Ruiter PC, Dong Q, Hastings A, Collins Johnson N,
622 McCann KS, Melville K, Morin PJ, Nadelhoffer K, Rosemond AD, Post DM, Sabo JL,
623 Scow KM, Vanni MJ, Wall DH (2004) Detritus, trophic dynamics and biodiversity. *Ecol*
624 *Lett* 7:584-600 doi:10.1111/j.1461-0248.2004.00606.x
- 625 Moriarty DJW (1982) Feeding of *Holothuria atra* and *Stichopus chloronotus* on bacteria, organic
626 carbon and nitrogen in sediments of the Great Barrier Reef. *Austral J Mar Freshw Res*
627 33:255-263 doi: 10.1071/MF9820255
- 628 Muscatine L (1973) Nutrition of corals. In: Jones OA, Endea R (eds) *Biology and Geology of*
629 *Coral Reefs* volume II. Academic Press, New York, pp 77-115
- 630 Muscatine L, Porter JW (1977) Reef corals: mutualistic symbioses adapted to nutrient-poor
631 conditions. *Bioscience* 27:454-460 doi:10.2307/1297526
- 632 Odum, H. T., and E. P. Odum. 1955. Trophic structure and productivity of a windward coral reef
633 community on Eniwetok Atoll. *Ecological Monographs* 25:291-320.
- 634 Pandolfi JM, Bradbury RH, Sala E, Hughes TP, Bjorndal KA, Cooke RG, McArdle D,
635 McClenachan L, Newman MJH, Paredes G, Warner RR, Jackson JBC (2003) Global
636 trajectories of the long-term decline of coral reef ecosystems. *Science* 301:955-958
637 doi:10.1126/science.1085706
- 638 Parnell AC, Inger R, Bearhop S, Jackson AL (2010) Source partitioning using stable isotopes:
639 Coping with too much variation. *PLOS One* 5:e9672 doi:10.1371/journal.pone.0009672.
- 640 Polovina JJ (1984) Model of a coral reef ecosystem I. the ECOPATH model and its application
641 to French Frigate Shoals. *Coral Reefs* 3:1-11 doi:10.1007/BF00306135

- 642 Post DM (2002) Using stable isotopes to estimate trophic position: models, methods, and
643 assumptions. *Ecology* 83:703-718 doi:10.1890/0012-
644 9658(2002)083[0703:USITET]2.0.CO;2
- 645 R Development Core Team (2013). R: A language and environment for statistical computing. R
646 Foundation for Statistical Computing, Vienna, Austria. ISBN 3-900051-07-0, URL
647 <http://www.R-project.org>.
- 648 Reeds P (2000) Dispensable and indispensable amino acids for humans. *J Nutr* 130:1835S-1840S
- 649 Richter C, Wunsch M, Rasheed M, Koetter I, Badran MI (2001) Endoscopic exploration of Red
650 Sea coral reefs reveals dense populations of cavity dwelling sponges. *Nature* 413:726–
651 730 doi:10.1038/35099547
- 652 Raubenheimer D, Simpson SJ, Mayntz D (2009) Nutrition, ecology and nutritional ecology:
653 toward an integrated framework. *Funct Ecol* 23:4-16 doi:10.1111/j.1365-
654 2435.2009.01522.x
- 655 Ryther JH (1969) Relationship of photosynthesis to fish production in the sea. *Science* 166:72-76
656 doi:10.1126/science.166.3901.72
- 657 Schiff JT, Batista FC, Sherwood OA, Guilderson TP, Hill TM, Ravelo AC, McMahon KW,
658 McCarthy MD (2014) Compound specific amino acid $\delta^{13}\text{C}$ patterns in a deep-sea
659 proteinaceous coral: implications for reconstructing detailed $\delta^{13}\text{C}$ records of exported
660 primary production. *Mar Chem* 166:82-91
- 661 Scott JH, O'Brien DM, Emerson D, Sun H, McDonald GD, Salgado A, Fogel M (2006) An
662 examination of the carbon isotope effects associated with amino acid biosynthesis.
663 *Astrobiology* 6:867-880 doi:10.1089/ast.2006.6.867

- 664 Sheppard CRC, Sheppard ALS (1991) Corals and coral communities of Arabia. *Fauna Saudi*
665 *Arabia* 12:7-192
- 666 Silfer JA, Engel MH, Macko SA, Jumeau EJ (1991) Stable carbon isotope analysis of amino-acid
667 enantiomers by conventional isotope ratio mass spectrometry and combined gas-
668 chromatography isotope ratio mass-spectrometry. *Anal Chem* 63:370-374
669 doi:10.1021/ac00004a014
- 670 Sommer C, Schneider W, Poutiers JM (1996) FAO species identification field guide for fishery
671 purposes. The living marine resources of Somalia. Food and Agricultural Organization of
672 the United Nations, Rome.
- 673 Uthicke S (1999) Sediment bioturbation and impact of feeding activity of *Holothuria*
674 (*Halodeima*) *atra* and *Stichopus chloronotus*, two sediment feeding holothurians, at
675 Lizard Island, Great Barrier Reef. *Bull Mar Sci* 64:129-141
- 676 Ward EJ, Semmens BX, Schindler DE (2010) Including source uncertainty and information in
677 the analysis of stable isotope mixing models. *Environ Sci Technol* 44:4645–4650
678 doi:10.1021/es100053v
- 679 Wild C, Huettel M, Kleute A, Kremb SG, Rasheed MYM, Jorgensen BB (2004) Coral mucus
680 functions as an energy carrier and particle trap in the reef ecosystem. *Nature* 428:66-70
681 doi:10.1038/nature02344
- 682 Wyatt AS, Lowe RJ, Humphries S, Waite AM (2010) Particulate nutrient fluxes over a fringing
683 coral reef: relevant scales of phytoplankton production and mechanisms of supply. *Mar*
684 *Ecol Prog Ser* 405:113-130 doi:10.3354/meps08508
- 685 Wyatt ASJ, Falter JL, Lowe RJ, Humphries S, Waite AM (2012a). Oceanographic forcing of
686 nutrient uptake and release over a fringing coral reef. *Limnol Oceanogr* 57:401-419

687 doi:10.4319/lo.2012.57.2.0401

688 Wyatt ASJ, Waite AM, Humphries S (2012b) Stable isotope analysis reveals community-level

689 variation in fish trophodynamics across a fringing coral reef. *Coral Reefs* 31:1029-1044

690 doi:10.1007/s00338-012-0923-y

691 Wyatt ASJ, Lowe RJ, Humphries S, Waite AM (2013) Particulate nutrient fluxes over a fringing

692 coral reef: Source-sink dynamics inferred from carbon to nitrogen ratios and stable

693 isotopes. *Limnol Oceanogr* 58:409-427 doi:10.4319/lo.2013.58.1.0409

Table 1. Results from a mixed-model analysis of variance (ANOVA) to test for variations in source end member $\delta^{13}\text{C}$ values of five essential amino acids (AAs) on Red Sea reefs. End-member (EM: plankton, macroalgae, coral, detritus) and location (Loc: shelf, oceanic) were fixed factors, while reef ($n = 4$) nested within location was a random factor. Bolded P values significant at $\alpha = 0.05$

AA	Source	SS	MS	df	F ratio	P < F
Threonine	Location	11.3	11.3	1,6	10.6	0.017
	EM	367.9	122.6	3,18	111.6	<0.0001
	Loc*EM	5.6	1.86	3,18	1.7	0.203
	Reef(Loc)	6.4	1.05	6,18	0.96	0.477
Isoleucine	Location	0.09	0.09	1,6	0.07	0.799
	EM	215.6	71.6	3,18	53.6	<0.0001
	Loc*EM	21.1	7.0	3,18	5.2	0.009
	Reef(Loc)	7.9	1.3	6,18	1.0	0.469
Valine	Location	4.8	4.8	1,6	6.4	0.045
	EM	392.0	130.7	3,18	246.2	<0.0001
	Loc*EM	16.1	5.4	3,18	10.1	0.0004
	Reef(Loc)	4.5	0.75	6,18	1.4	0.26
Phenylalanine	Location	2.1	2.1	1,6	1.6	0.254
	EM	194.0	64.7	3,18	60.4	<0.0001
	Loc*EM	2.1	0.7	3,18	0.7	0.59
	Reef(Loc)	7.9	1.3	6,18	1.2	0.34
Leucine	Location	0.9	0.9	1,6	0.5	0.487
	EM	441.2	147.1	3,18	196.9	<0.0001
	Loc*EM	6.3	2.1	3,18	2.8	0.069
	Reef(Loc)	10.4	1.7	6,18	2.3	0.077

Table 2. Eigenvectors and variance explained (%) for the five principal components (PC) in the principal component analysis of $\delta^{13}\text{C}$ values from end member (plankton, macroalgae, coral, and detritus) essential amino acids on shelf and oceanic reefs near Al-Lith, Saudi Arabia in the Red Sea

	PC1	PC2	PC3	PC4	PC5
Threonine	-0.46	0.35	0.68	0.38	-0.23
Isoleucine	-0.33	0.70	-0.24	-0.58	0.07
Valine	-0.42	-0.54	0.12	-0.52	-0.50
Phenylalanine	-0.50	-0.03	-0.67	0.50	-0.21
Leucine	-0.50	-0.31	0.11	-0.03	0.80
Variance	69.5	23.1	3.9	2.5	1.1

Table 3. Eigenvectors and variance explained (%) for the five principal components (PC) in the principal component analysis of end member and fish essential amino acid $\delta^{13}\text{C}$ values from shelf and oceanic reefs near Al-Lith, Saudi Arabia in the Red Sea

	PC1		PC2		PC3		PC4		PC5	
	shelf	oceanic	shelf	oceanic	shelf	oceanic	shelf	oceanic	shelf	oceanic
Threonine	0.56	0.44	-0.39	0.50	-0.68	-0.74	0.25	0.06	0.11	0.07
Isoleucine	0.38	0.24	-0.63	0.57	0.56	0.57	-0.35	0.54	0.17	-0.01
Valine	0.41	0.45	0.55	-0.58	0.16	-0.04	0.06	0.54	0.70	0.40
Phenylalanine	0.38	0.43	0.11	0.13	0.42	0.35	0.66	-0.60	-0.47	0.56
Leucine	0.48	0.60	0.38	-0.26	-0.13	0.10	-0.61	-0.23	-0.49	-0.72
Variance (%)	63.3	69.9	28.0	21.9	4.4	4.1	2.9	2.5	1.5	1.4

FIGURES

Fig. 1 Map of the collection sites for source end-members and fish species from shelf reefs (triangles) located on the continental shelf and oceanic reefs (circles) located off the continental shelf and surrounded by deep open water (four reefs per location) near Al-Lith (star symbol in inset), Saudi Arabia in the Red Sea. Contour lines indicate 25m isobaths

Fig. 2 Multivariate separation of four source end-members on reefs along the Saudi Arabian coast of the Red Sea visualized as principal component 1 and 2 of a principal component analysis of the $\delta^{13}\text{C}$ values of five essential amino acid: threonine, isoleucine, valine, phenylalanine, and leucine. Samples were analyzed from shelf reefs (filled symbols) and oceanic reefs (open symbols) and plotted with 95% confidence ellipses. The four source end-members were: plankton (blue diamonds), macroalgae (green circles), coral (magenta triangles), and detritus (brown squares)

Fig. 3 Multivariate separation of seven reef fish species and four source end-members, visualized as the first 3 principal components of a principal component analysis of the $\delta^{13}\text{C}$ values of five essential amino acid: threonine, isoleucine, valine, phenylalanine, and leucine. The four source end-members were plotted as 95% confidence ellipses as follows: plankton (blue), macroalgae (green), coral (magenta), and detritus (brown). Symbols for primary consumers of each of the four end-members were filled in the same color as the 95% confidence ellipses of their diet end-member: *Amblyglyphidodon indicus* (blue diamonds), *Stegastes nigricans* (green circles), *Chaetodon trifascialis* (magenta triangles) and *Ctenochaetus striatus* (brown squares). The remaining species (open symbols) were *Chlorurus sordidus* (red triangles), *Lutjanus ehrenbergii* (purple squares), and *Gymnothorax javanicus* (cyan diamonds) (n = 20 individuals per species per location except *G. javanicus* where n = 10 individuals per location)

Fig. 4 Relative contributions of four source end-members, plankton (blue), macroalgae (green), coral (magenta), and detritus (brown) to the dietary carbon supporting seven fish species, *Stegastes nigricans*, *Chaetodon trifascialis*, *Ctenochaetus striatus*, *Chlorurus sordidus*, *Amblyglyphidodon indicus*, *Lutjanus ehrenbergii*, and *Gymnothorax javanicus*, from a) shelf reefs and b) oceanic reefs near Al-Lith, Saudi Arabia in the Red Sea. Relative contributions were determined from the $\delta^{13}\text{C}$ values of five essential amino acids (threonine, isoleucine, valine, phenylalanine, and leucine) of end-members and consumers using a Bayesian stable isotope mixing model (bars represent individuals, n = 20 individuals per species per location except *G. javanicus* where n = 10 individuals per location)

Fig. 5 Constellation plot identifying six clusters (A-F) determined from a k-means cluster analysis of the relative contributions of four source end-members to seven coral reef fish species, *Stegastes nigricans* (Sni), *Amblyglyphidodon indicus* (Ain), *Ctenochaetus striatus* (Cst), *Chlorurus sordidus* (Sor), *Chaetodon trifascialis* (Ctr), *Lutjanus ehrenbergii* (Leh), and *Gymnothorax javanicus* (Gja) collected from shelf reefs (purple labels) and oceanic reefs (cyan labels) along the Saudi Arabian coast of the Red Sea. Points represent individuals (n = 20 individuals per species per location except *G. javanicus* where n = 10 individuals per location). Symbol color shows dominant end-member: phytoplankton (blue symbols), macroalgae (green symbols), coral (magenta symbols), and detritus (brown symbols) for each fish sample

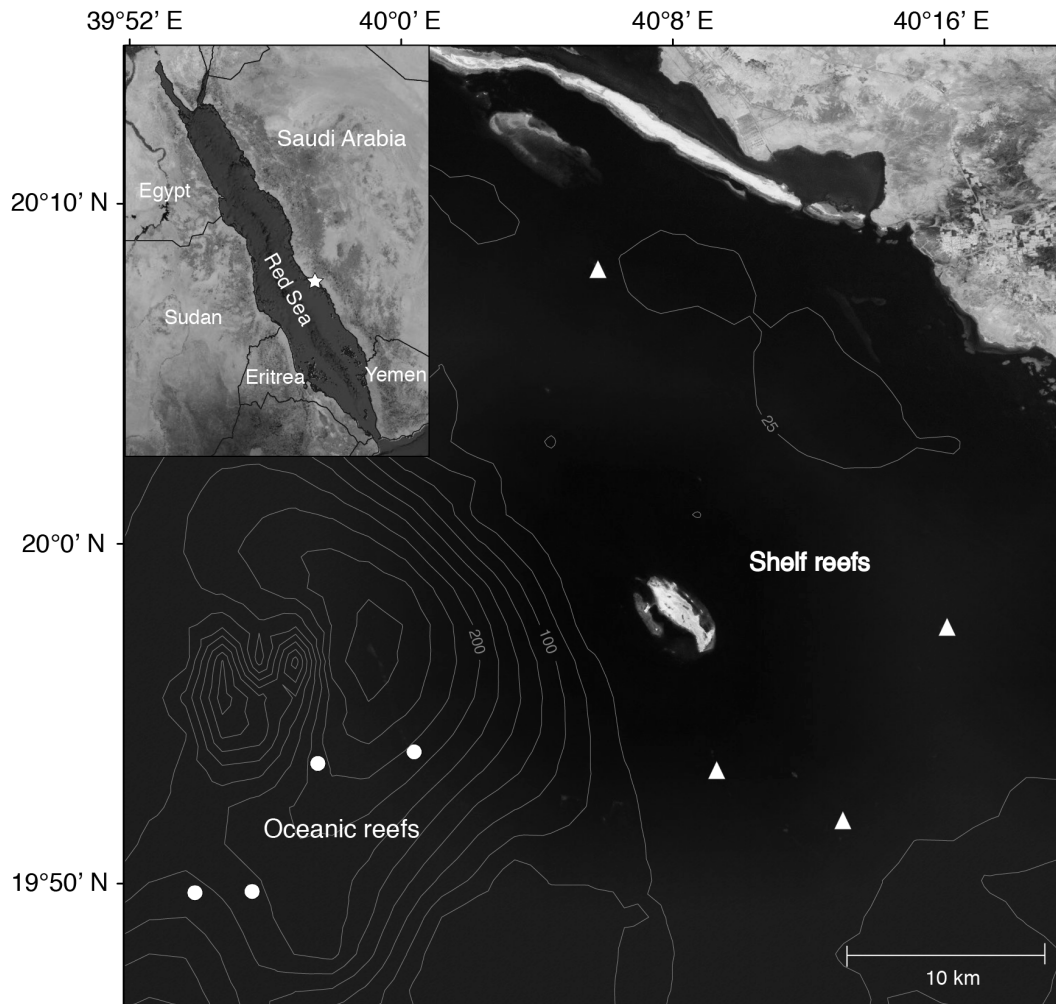


Figure 1.

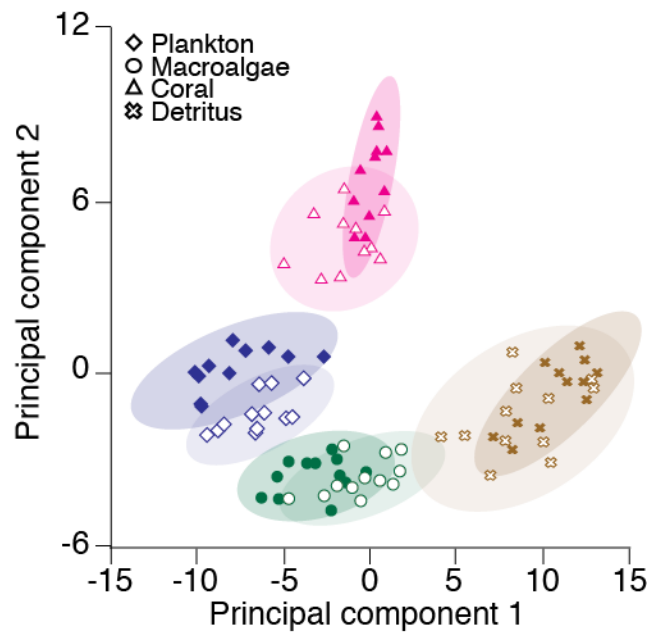


Figure 2

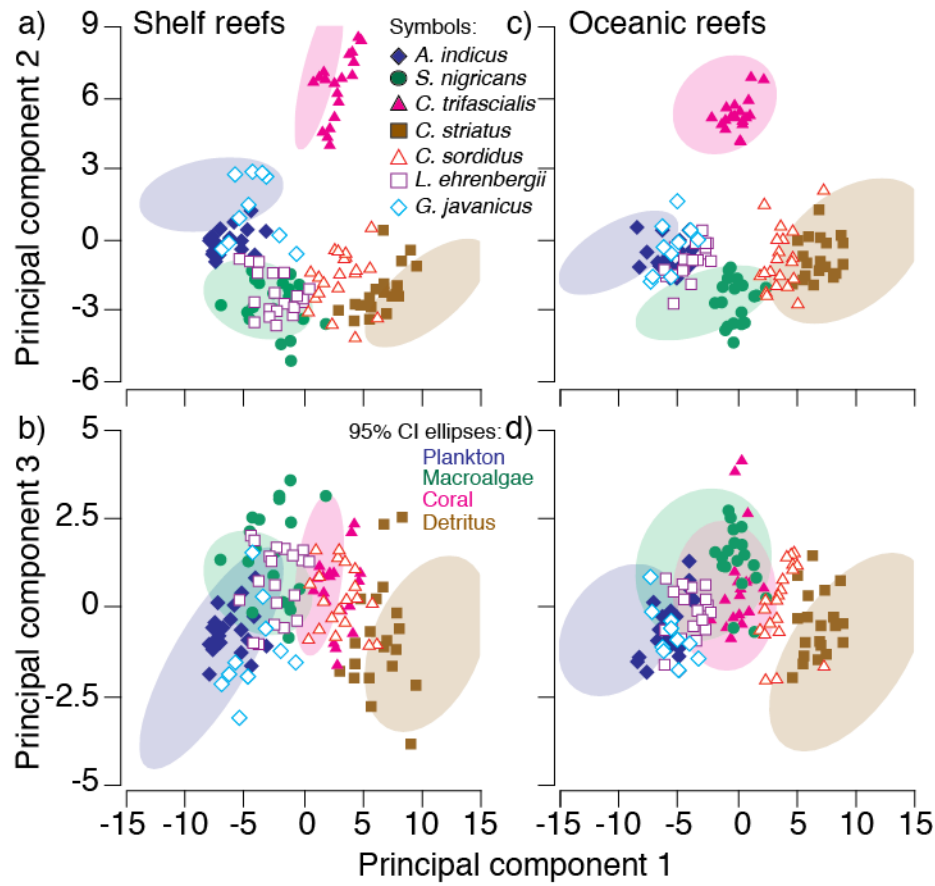


Figure 3.

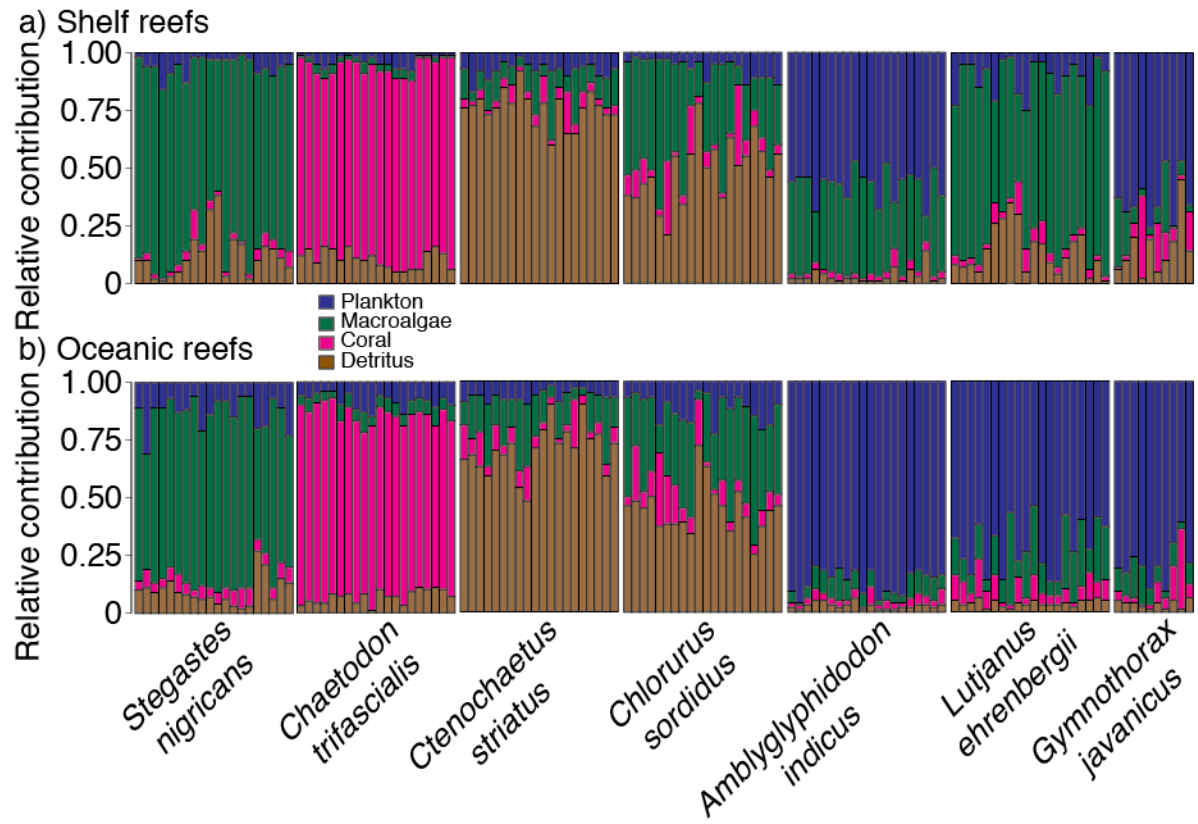


Figure 4.

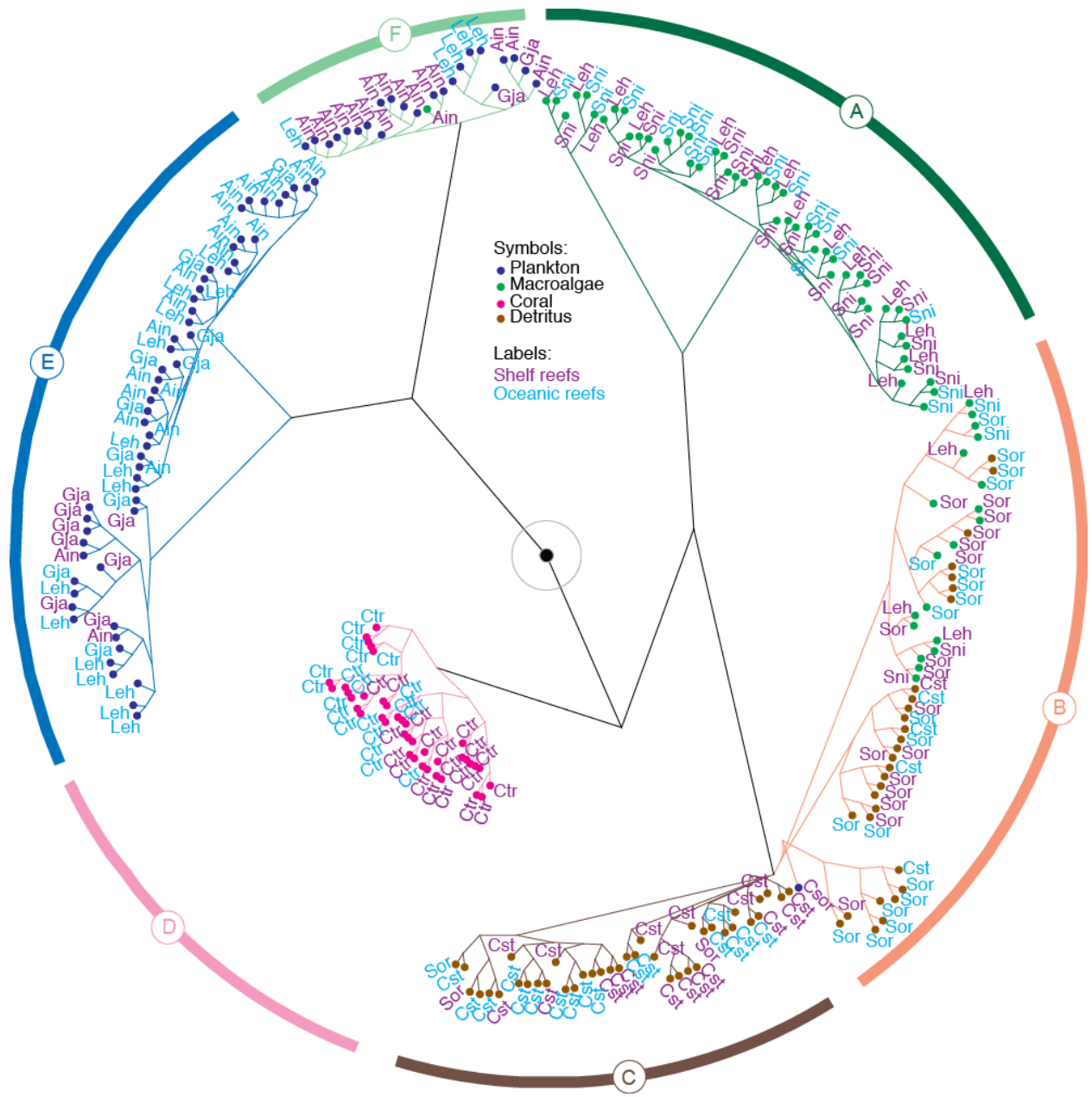


Figure 5.

Running Head: Carbon flow in tropical seascapes

Tracing carbon flow through coral reef food webs using a compound-specific stable isotope
approach

Kelton W. McMahon^{1,2,*#}, Simon R. Thorrold², Leah A. Houghton², Michael L. Berumen¹

¹Red Sea Research Center, Division of Biological and Environmental Science and Engineering,
King Abdullah University of Science and Technology, Thuwal, 23955, Saudi Arabia

²Biology Department, Woods Hole Oceanographic Institution, Woods Hole, MA 02543, USA

*Author of correspondence: Email: kmcmahon@whoi.edu

#Current address: Ocean Sciences Department, University of California - Santa Cruz, Santa Cruz,
CA, 95064, USA

Declaration of Authorship: KWM, SRT, and MLB conceived of and designed the study, KWM and MLB conducted the fieldwork, KWM and LAH conducted the laboratory analyses, KWM and SRT analyzed the data and wrote the manuscript, MLB and LAH revised and edited the manuscript.

Conflict of Interest: The authors declare that they have no conflict of interest.

Online Resource 1. Total length (mean \pm SD measured to the nearest 1mm) of seven species of coral reef fishes analyzed for essential amino acid $\delta^{13}\text{C}$ values from shelf and oceanic reefs near Al-Lith, Saudi Arabia in the Red Sea (n = 20 individuals per location). Statistical differences in mean total length were determined by a Welch's unequal variances t-test. Total lengths were not collected for *G. javanicus*, but all individuals were $> 1\text{m}$ and considered adults

	Mean Shelf	Mean Oceanic	$T_{df=38}$ (P value)
<i>L. ehrenbergii</i>	211 \pm 16	208 \pm 19	0.57 ($P = 0.58$)
<i>C. striatus</i>	140 \pm 17	142 \pm 16	-0.37 ($P = 0.71$)
<i>C. sordidus</i>	167 \pm 26	174 \pm 39	-0.59 ($P = 0.56$)
<i>A. indicus</i>	89 \pm 15	91 \pm 14	-0.49 ($P = 0.63$)
<i>C. trifascialis</i>	107 \pm 11	110 \pm 9	-0.87 ($P = 0.39$)
<i>S. nigricans</i>	99 \pm 11	93 \pm 12	1.48 ($P = 0.15$)
<i>G. javanicus</i>	-	-	-

Online Resource 2. Mean ($\% \pm$ SD) essential amino acid $\delta^{13}\text{C}$ values of four source end-members and seven coral reef fish species collected from four shelf reefs and four oceanic reefs (Location: Latitude, Longitude) ($n = 3$ for all source end-members, 5 for all fish species except *G. javanicus* where $n = 2$ for Ron's reef, Saut reef, Shi'b Sulaym reef, and Dohra reef, and $n = 3$ for LJ's reef, Brown reef, Canyon reef, and MarMar reef)

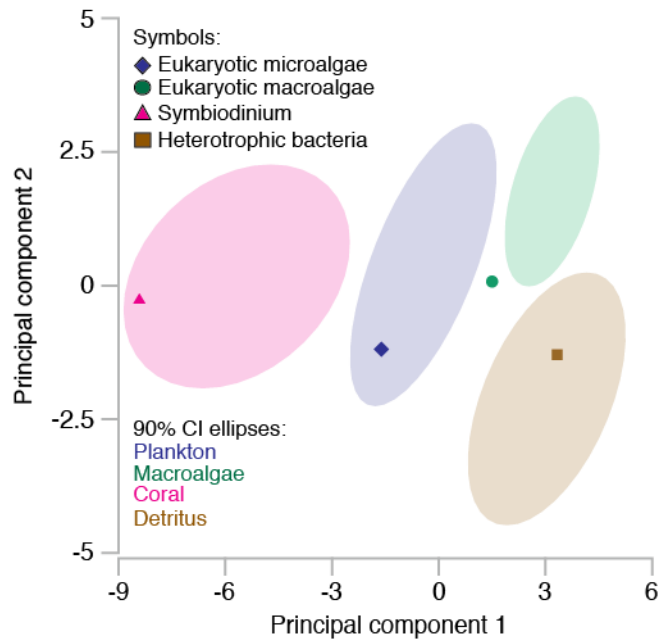
	Threonine	Isoleucine	Valine	Phenylalanine	Leucine
Ron's Reef (Shelf: 20.1348°N, 40.1012°W)					
Plankton	-9.6 \pm 0.5	-17.8 \pm 0.5	-23.2 \pm 0.3	-24.7 \pm 0.4	-25.5 \pm 0.2
Macroalgae	-9.7 \pm 0.8	-16.2 \pm 0.9	-18.3 \pm 0.8	-21.1 \pm 1.0	-22.7 \pm 1.1
Coral	-1.8 \pm 0.6	-7.8 \pm 0.5	-22.1 \pm 0.3	-19.3 \pm 0.4	-23.3 \pm 0.6
Detritus	0.1 \pm 1.2	-10.4 \pm 0.7	-12.1 \pm 0.7	-16.1 \pm 0.4	-13.9 \pm 0.7
<i>L. ehrenbergii</i>	-8.7 \pm 0.8	-16.7 \pm 0.8	-18.9 \pm 1.2	-21.1 \pm 1.0	-20.8 \pm 0.5
<i>C. striatus</i>	-0.6 \pm 1.8	-12.6 \pm 0.5	-13.9 \pm 0.5	-17.7 \pm 0.4	-15.6 \pm 0.4
<i>C. sordidus</i>	-4.5 \pm 1.5	-13.7 \pm 0.9	-16.2 \pm 1.1	-17.6 \pm 0.6	-20.1 \pm 0.6
<i>A. indicus</i>	-9.5 \pm 0.5	-17.1 \pm 0.5	-20.9 \pm 0.3	-23.2 \pm 0.2	-23.8 \pm 0.1
<i>C. trifascialis</i>	-0.3 \pm 0.2	-9.6 \pm 1.2	-20.8 \pm 0.3	-18.7 \pm 0.1	-22.3 \pm 0.5
<i>S. nigricans</i>	-10.7 \pm 0.9	-16.3 \pm 1.1	-18.1 \pm 1.5	-20.7 \pm 0.9	-20.8 \pm 1.3
<i>G. javanicus</i>	-8.2 \pm 0.1	-17.6 \pm 0.3	-21.0 \pm 0.1	-23.6 \pm 0.4	-23.3 \pm 0.1
LJ's Reef (Shelf: 19.9582°N, 40.2673°W)					
Plankton	-8.0 \pm 0.2	-17.9 \pm 0.4	-23.2 \pm 0.3	-24.9 \pm 0.2	-26.6 \pm 0.3
Macroalgae	-10.7 \pm 1.1	-17.0 \pm 0.9	-19.4 \pm 0.4	-22.2 \pm 0.3	-21.7 \pm 0.8
Coral	-4.1 \pm 0.9	-9.3 \pm 1.1	-21.2 \pm 0.4	-18.7 \pm 0.3	-22.3 \pm 0.4
Detritus	-1.2 \pm 1.7	-13.8 \pm 1.4	-14.3 \pm 0.2	-17.1 \pm 0.6	-14.5 \pm 1.3
<i>L. ehrenbergii</i>	-8.4 \pm 1.4	-16.3 \pm 0.5	-18.5 \pm 1.2	-20.7 \pm 1.0	-21.5 \pm 0.8
<i>C. striatus</i>	-2.6 \pm 0.9	-15.1 \pm 1.1	-15.3 \pm 0.7	-17.9 \pm 0.4	-16.8 \pm 0.7
<i>C. sordidus</i>	-6.3 \pm 0.6	-14.5 \pm 1.1	-17.1 \pm 1.4	-19.1 \pm 1.0	-18.4 \pm 1.3
<i>A. indicus</i>	-9.4 \pm 0.4	-17.6 \pm 0.3	-21.4 \pm 0.3	-23.5 \pm 0.3	-24.1 \pm 0.3
<i>C. trifascialis</i>	-3.2 \pm 0.3	-10.4 \pm 0.4	-20.4 \pm 0.3	-18.1 \pm 0.4	-21.5 \pm 0.3
<i>S. nigricans</i>	-9.8 \pm 1.1	-15.4 \pm 0.6	-18.1 \pm 0.6	-21.2 \pm 1.0	-21.7 \pm 0.6
<i>G. javanicus</i>	-6.4 \pm 0.2	-16.3 \pm 0.7	-21.8 \pm 1.1	-22.8 \pm 0.7	-23.6 \pm 1.3
Saut Reef (Shelf: 19.8875°N, 40.1565°W)					
Plankton	-7.7 \pm 0.4	-14.0 \pm 1.1	-21.0 \pm 1.1	-23.8 \pm 1.0	-23.3 \pm 0.9
Macroalgae	-8.7 \pm 1.0	-16.7 \pm 0.7	-17.6 \pm 0.5	-19.3 \pm 0.2	-20.3 \pm 0.2
Coral	-3.6 \pm 0.7	-9.5 \pm 1.2	-22.3 \pm 0.9	-21.3 \pm 1.3	-21.5 \pm 0.8
Detritus	0.6 \pm 1.6	-11.7 \pm 0.8	-12.3 \pm 0.4	-16.6 \pm 0.9	-14.1 \pm 0.9
<i>L. ehrenbergii</i>	-7.9 \pm 0.7	-15.1 \pm 0.3	-16.8 \pm 0.4	-19.0 \pm 0.7	-20.1 \pm 0.6
<i>C. striatus</i>	-3.3 \pm 0.9	-11.6 \pm 1.5	-14.0 \pm 0.6	-17.2 \pm 1.0	-17.4 \pm 0.6
<i>C. sordidus</i>	-4.1 \pm 1.5	-13.7 \pm 1.6	-15.2 \pm 1.2	-18.1 \pm 0.6	-17.1 \pm 1.1
<i>A. indicus</i>	-8.4 \pm 1.1	-15.5 \pm 0.4	-19.8 \pm 0.5	-22.5 \pm 0.4	-22.0 \pm 0.6
<i>C. trifascialis</i>	-3.3 \pm 0.6	-8.0 \pm 0.4	-21.5 \pm 0.2	-21.5 \pm 0.6	-21.2 \pm 0.3
<i>S. nigricans</i>	-9.5 \pm 1.3	-15.4 \pm 1.1	-15.9 \pm 0.7	-18.4 \pm 0.7	-19.7 \pm 0.8
<i>G. javanicus</i>	-6.1 \pm 0.1	-14.1 \pm 1.5	-19.7 \pm 0.5	-22.5 \pm 1.2	-22.0 \pm 1.2
Brown Reef (Shelf: 19.8556°N, 40.2162°W)					

Plankton	-7.8 ± 0.6	-16.3 ± 0.5	-22.9 ± 0.1	-23.8 ± 0.8	-24.8 ± 0.3
Macroalgae	-7.7 ± 0.8	-17.3 ± 0.8	-18.0 ± 0.6	-19.5 ± 1.0	-22.4 ± 0.4
Coral	-2.1 ± 0.3	-7.9 ± 0.5	-21.3 ± 0.6	-19.3 ± 0.8	-23.1 ± 0.3
Detritus	-0.3 ± 1.2	-11.4 ± 1.7	-12.3 ± 1.7	-16.5 ± 1.3	-15.3 ± 0.7
<i>L. ehrenbergii</i>	-8.0 ± 1.3	-16.3 ± 0.3	-17.6 ± 0.9	-19.3 ± 0.6	-22.1 ± 2.1
<i>C. striatus</i>	-2.9 ± 1.2	-13.9 ± 0.4	-14.3 ± 0.8	-18.3 ± 1.4	-16.4 ± 0.5
<i>C. sordidus</i>	-4.3 ± 1.2	-13.3 ± 0.9	-16.1 ± 1.0	-18.4 ± 0.3	-18.2 ± 0.5
<i>A. indicus</i>	-7.9 ± 0.9	-16.1 ± 0.7	-20.5 ± 0.5	-22.5 ± 0.7	-23.4 ± 0.6
<i>C. trifascialis</i>	-1.0 ± 0.7	-6.7 ± 1.0	-20.0 ± 0.6	-19.0 ± 0.5	-22.3 ± 0.4
<i>S. nigricans</i>	-6.5 ± 0.4	-16.2 ± 0.7	-17.0 ± 0.5	-19.2 ± 0.6	-21.9 ± 0.6
<i>G. javanicus</i>	-7.1 ± 1.4	-13.3 ± 1.2	-20.1 ± 2.1	-22.5 ± 0.7	-21.7 ± 1.8
Canyon Reef (Oceanic: 19.8923°N, 39.9591°W)					
Plankton	-10.4 ± 1.0	-16.6 ± 0.8	-20.5 ± 1.3	-24.1 ± 0.5	-25.3 ± 0.3
Macroalgae	-9.6 ± 1.0	-14.5 ± 1.0	-16.5 ± 1.0	-19.2 ± 1.7	-19.4 ± 0.9
Coral	-5.5 ± 1.3	-12.2 ± 0.9	-22.1 ± 1.2	-18.0 ± 0.4	-22.1 ± 0.8
Detritus	-1.8 ± 1.6	-11.7 ± 0.5	-13.3 ± 1.1	-16.4 ± 1.7	-14.6 ± 1.7
<i>L. ehrenbergii</i>	-9.4 ± 0.5	-16.2 ± 0.9	-19.4 ± 0.5	-22.4 ± 1.0	-24.0 ± 0.4
<i>C. striatus</i>	-3.7 ± 1.0	-12.4 ± 0.8	-14.5 ± 0.5	-17.4 ± 0.4	-16.9 ± 0.8
<i>C. sordidus</i>	-6.0 ± 0.9	-12.7 ± 0.6	-15.7 ± 1.5	-18.0 ± 0.9	-18.0 ± 0.9
<i>A. indicus</i>	-9.7 ± 0.5	-16.5 ± 0.6	-21.4 ± 1.0	-24.5 ± 0.7	-24.3 ± 0.9
<i>C. trifascialis</i>	-5.2 ± 2.0	-7.9 ± 0.2	-20.7 ± 0.6	-19.5 ± 0.4	-21.3 ± 0.1
<i>S. nigricans</i>	-8.9 ± 1.1	-15.1 ± 1.7	-16.7 ± 1.0	-20.7 ± 0.9	-19.0 ± 1.0
<i>G. javanicus</i>	-10.9 ± 1.0	-15.9 ± 0.5	-20.3 ± 1.1	-24.1 ± 0.3	-23.7 ± 0.3
Shi'b Sulaym Reef (Oceanic: 19.8980°N, 40.0062°W)					
Plankton	-9.6 ± 1.0	-16.1 ± 0.2	19.9 ± 0.9	-23.4 ± 0.7	-24.8 ± 0.4
Macroalgae	-10.4 ± 1.2	-15.6 ± 0.7	-17.3 ± 1.3	-20.1 ± 1.3	20.4 ± 0.8
Coral	-3.7 ± 1.4	-11.0 ± 0.5	-22.4 ± 0.6	-18.7 ± 0.5	-21.5 ± 0.6
Detritus	-0.7 ± 0.5	-12.1 ± 1.6	-13.4 ± 0.8	-16.9 ± 1.9	-14.8 ± 1.7
<i>L. ehrenbergii</i>	-10.0 ± 1.0	-15.6 ± 0.6	-19.1 ± 0.5	-22.7 ± 0.5	-23.5 ± 0.7
<i>C. striatus</i>	-3.8 ± 0.9	-13.2 ± 0.4	-15.2 ± 1.0	-17.5 ± 0.7	-15.9 ± 1.1
<i>C. sordidus</i>	-5.0 ± 2.1	-13.6 ± 0.8	-16.4 ± 0.8	-17.8 ± 1.4	-18.8 ± 0.5
<i>A. indicus</i>	-9.2 ± 0.8	-16.0 ± 0.4	-19.2 ± 0.3	-23.2 ± 0.6	-24.0 ± 0.4
<i>C. trifascialis</i>	-4.3 ± 0.5	-11.3 ± 0.3	-21.3 ± 0.4	-19.5 ± 0.8	-21.6 ± 0.5
<i>S. nigricans</i>	-10.3 ± 0.4	-15.3 ± 0.5	-16.9 ± 0.8	-20.4 ± 0.8	-20.1 ± 0.6
<i>G. javanicus</i>	-9.2 ± 0.1	-16.4 ± 0.3	-20.9 ± 1.2	-22.8 ± 1.0	-23.9 ± 0.9
MarMar Reef (Oceanic: 19.8296°N, 39.9267°W)					
Plankton	-8.8 ± 0.5	-15.6 ± 1.4	-19.9 ± 1.1	-22.4 ± 0.4	-24.0 ± 0.8
Macroalgae	-7.8 ± 0.7	-14.6 ± 0.6	-16.6 ± 0.9	-20.5 ± 0.6	-20.7 ± 0.8
Coral	-4.6 ± 1.2	-9.8 ± 0.8	-22.1 ± 0.2	-21.5 ± 0.5	-23.9 ± 0.5
Detritus	-3.5 ± 0.6	-13.8 ± 0.4	-14.4 ± 0.5	-18.4 ± 1.2	-16.7 ± 1.6
<i>L. ehrenbergii</i>	-8.6 ± 0.6	-14.5 ± 0.5	-18.7 ± 0.5	-22.0 ± 0.4	-23.2 ± 1.0
<i>C. striatus</i>	-4.4 ± 0.7	-13.4 ± 1.2	-14.5 ± 0.6	-18.7 ± 0.4	-17.6 ± 0.7
<i>C. sordidus</i>	-5.6 ± 0.5	-14.2 ± 0.8	-15.2 ± 0.6	-19.9 ± 0.7	-19.0 ± 0.8

<i>A. indicus</i>	-9.7 ± 0.8	-16.7 ± 0.5	-21.6 ± 0.7	-22.4 ± 0.3	-23.6 ± 0.2
<i>C. trifascialis</i>	-4.7 ± 0.6	-10.7 ± 0.3	-21.1 ± 0.1	-21.2 ± 0.4	-22.6 ± 0.6
<i>S. nigricans</i>	-9.3 ± 0.5	-13.4 ± 0.5	-16.9 ± 0.5	-20.0 ± 0.5	-20.9 ± 0.2
<i>G. javanicus</i>	-8.1 ± 0.5	-16.0 ± 0.8	-20.7 ± 0.9	-22.2 ± 0.8	-24.0 ± 0.3
Dohra Reef (Oceanic: 19.8289°N, 39.8987°W)					
Plankton	-8.6 ± 0.6	-14.4 ± 0.7	-19.8 ± 1.1	-22.0 ± 0.7	-24.4 ± 0.3
Macroalgae	-8.7 ± 1.2	-14.3 ± 0.9	-16.0 ± 0.9	-19.6 ± 1.1	-19.5 ± 0.8
Coral	-5.5 ± 0.8	-11.1 ± 1.4	-22.1 ± 0.9	-19.0 ± 1.6	-23.1 ± 1.5
Detritus	-2.5 ± 2.1	-12.5 ± 1.9	-13.1 ± 0.5	-15.4 ± 1.0	-14.0 ± 1.7
<i>L. ehrenbergii</i>	-8.4 ± 0.9	-14.9 ± 0.5	-18.7 ± 0.4	-21.2 ± 0.3	-22.7 ± 0.6
<i>C. striatus</i>	-5.5 ± 2.7	-11.2 ± 2.6	-14.0 ± 0.4	-15.9 ± 1.8	-15.0 ± 1.5
<i>C. sordidus</i>	-6.4 ± 0.7	-12.7 ± 0.9	-15.1 ± 0.3	-18.7 ± 0.8	-18.6 ± 1.0
<i>A. indicus</i>	-9.3 ± 0.5	-14.3 ± 0.4	-18.6 ± 0.5	-21.9 ± 0.2	-23.7 ± 0.2
<i>C. trifascialis</i>	-4.8 ± 0.3	-11.3 ± 0.4	-21.0 ± 0.2	-17.7 ± 0.2	-22.5 ± 0.5
<i>S. nigricans</i>	-8.4 ± 1.1	-14.3 ± 0.3	-16.4 ± 0.8	-19.8 ± 0.5	-18.9 ± 0.6
<i>G. javanicus</i>	-7.5 ± 0.2	-15.5 ± 0.3	-20.2 ± 1.1	-21.3 ± 0.3	-24.2 ± 1.4

Online Resource 3. Mean individual variance ($\% \pm \text{SD}$) in SIAR model output of relative contribution of four source end-members to seven coral reef fish species on shelf and oceanic reefs near Al-Lith, Saudi Arabia in the Red Sea ($n = 20$ individual per location, except *G. javanicus* where $n = 10$ individuals per location). The standard deviation in relative contribution for each individual was calculated from 500,000 iterations of the model with a 50,000 burn-in discard and then averaged for each location ($n = 4$ reefs per location, consisting of 5 individuals per reef for all species except *G. javanicus* where two to three individuals were used per reef)

	Plankton SD		Macroalgae SD		Coral SD		Detritus SD	
	shelf	oceanic	shelf	oceanic	shelf	oceanic	shelf	oceanic
<i>L. ehrenbergii</i>	5.7 ± 2.5	7.9 ± 2.4	8.1 ± 2.9	8.5 ± 2.5	3.1 ± 1.2	5.0 ± 2.1	4.0 ± 1.5	3.1 ± 0.9
<i>C. striatus</i>	4.7 ± 1.4	4.9 ± 1.5	6.5 ± 2.0	8.3 ± 2.6	3.3 ± 1.4	4.3 ± 2.0	4.1 ± 0.9	6.5 ± 1.7
<i>C. sordidus</i>	5.0 ± 2.3	7.5 ± 2.2	7.8 ± 2.5	11.8 ± 3.0	3.7 ± 1.4	5.0 ± 2.1	4.4 ± 0.7	7.7 ± 1.7
<i>A. indicus</i>	5.7 ± 1.5	4.9 ± 1.4	6.3 ± 1.7	4.9 ± 1.8	2.1 ± 1.0	2.8 ± 1.2	1.8 ± 0.9	2.0 ± 0.7
<i>C. trifascialis</i>	2.5 ± 1.6	5.3 ± 1.4	2.1 ± 1.0	4.7 ± 0.9	4.4 ± 1.1	6.1 ± 1.1	3.3 ± 0.5	4.1 ± 1.6
<i>S. nigricans</i>	4.0 ± 2.1	7.8 ± 2.0	6.2 ± 1.9	10.5 ± 3.2	2.6 ± 1.1	4.5 ± 1.0	3.5 ± 1.3	5.4 ± 2.2
<i>G. javanicus</i>	6.3 ± 2.9	7.6 ± 4.2	6.3 ± 3.9	6.2 ± 2.5	3.9 ± 2.7	5.1 ± 4.6	3.2 ± 1.0	2.6 ± 0.9



Online Resource 4. Normalized $\delta^{13}\text{C}$ fingerprints of five essential amino acids (threonine, isoleucine, valine, phenylalanine, and leucine) from carbon source end-members visualized using a principal components analysis (PCA). Samples of end-members ($n = 24$) from reefs near Al-Lith, Saudi Arabia in the Red Sea 90% are displayed as 90% probability ellipses and color-coded as follows: phytoplankton (blue), macroalgae (green), coral (magenta), and detritus (brown). Reference end-members are plotted as filled symbols and include eukaryotic microalgae (blue diamonds), eukaryotic macroalgae (green circles), *Symbiodinium* sp. (magenta triangles), and heterotrophic bacteria (brown squares). The eukaryotic microalgae comprised diatoms, chrysophytes, and chlorophytes from Larsen et al. (2013). The eukaryotic macroalgae comprise Rhodophytes in the same class as the Red Sea macroalgae, Florideophyceae, from Larsen et al. (2013). The *Symbiodinium* sp. samples were isolated from a pure culture at Woods Hole Oceanographic Institution. The heterotrophic bacteria comprise *Rhodococcus spp.* from Larsen et al. (2013)